

# Stochastic models of gene transcription with upstream drives: Exact solution and sample path characterisation

Justine Dattani and Mauricio Barahona\*

Department of Mathematics  
Imperial College London  
London SW7 2AZ, United Kingdom

## Abstract

Gene transcription is a highly stochastic and dynamic process. As a result, the mRNA copy number of a given gene is heterogeneous both between cells and across time. We present a framework to model gene transcription in populations of cells with time-varying (stochastic or deterministic) transcription and degradation rates. Such rates can be understood as upstream cellular drives representing the effect of different aspects of the cellular environment. We show that the full solution of the master equation contains two components: a model-specific, upstream effective drive, which encapsulates the effect of cellular drives (e.g., entrainment, periodicity or promoter randomness), and a downstream transcriptional Poissonian part, which is common to all models. Our analytical framework treats cell-to-cell and dynamic variability consistently, unifying several approaches in the literature. We apply the obtained solution to characterise different models of experimental relevance, and to explain the influence on gene transcription of synchrony, stationarity, ergodicity, as well as the effect of time-scales and other dynamic characteristics of drives. We also show how the solution can be applied to the analysis of noise sources in single-cell data, and to reduce the computational cost of stochastic simulations.

## 1 Introduction

Gene transcription, the cellular mechanism through which DNA is copied into mRNA transcripts, is a complex, stochastic process involving small numbers of molecules [30]. As a result, the number of mRNA copies for most genes is highly heterogeneous over time within each cell, and across cells in a population [46, 37, 55]. Such fundamental randomness is biologically relevant: it underpins the cell-to-cell variability linked with phenotypic outcomes and cell decisions [32, 7, 3, 14, 72].

The full mathematical analysis of gene expression variability requires the solution of *master equations*. Given a gene transcription model, its master equation (ME) is a differential-difference equation that describes the evolution of  $P(n, t)$ , the probability of having  $n$  mRNA molecules in a single cell at time  $t$ . However, MEs are problematic to solve, both analytically and numerically, due to the difficulties associated with discrete stochastic variables—the molecule number  $n$  is an integer [71]. Most existing analytical

---

\*m.barahona@imperial.ac.uk

solutions of the ME are specific to particular models and are typically obtained via the probability generating function under stationarity assumptions [20, 70, 76, 44, 28]. A few other solutions include the decaying time-dependence describing the relaxation transient towards stationarity from a given initial distribution [21, 54, 69, 58]. In the usual situation when analytical solutions are intractable, the first few moments of the distribution are approximated, usually at stationarity, although error bounds are difficult to obtain under closure schemes [40, 50]. Alternatively, full stochastic simulations are used, yet the computational cost to sample  $P(n, t)$  at each  $t$  is often impractical, and many methods lead to estimation bias in practice [75].

The emergence of accurate time-course measurements of mRNA counts in single cells [37, 9, 38, 55, 73] has revealed the high dynamic variability of gene expression both at the single-cell and population levels. This variability has several sources. Cells express genes heterogeneously [25, 55] and hence models need to capture intercellular variability; but cells are also subjected to time-varying inputs of a stochastic and/or deterministic nature, either from their environment or from regulatory gene networks inside the cell. Therefore, standard ME models with stationary solutions, which also tacitly assume that gene expression is uncorrelated between cells, cannot capture fully such sources of variability. Mathematically, ME models must be able to describe time-dependent gene transcription in single cells within an inhomogeneous population, i.e., they must allow a varying degree of synchrony and of cell-to-cell variability across the population. In addition, they must be able to account for non-stationary dynamic variability due to upstream biological drives, such as circadian rhythms and cell cycle [33, 4], external signalling [8], or stimulus-induced modulation or entrainment [34, 27].

Recent techniques to model cell-to-cell correlations have used the marginalisation of extrinsic components [74], mixed-effects models [2], or deterministic rate parameters [24]. Several of the results correspond to deterministic rates and are well-known in queuing theory [11]. However, full solutions of the ME that capture temporal heterogeneity as well as variability in parameters, from the single-cell to the population level, are yet to be explored, and could help unravel conjunctly with experiments how the dynamics of upstream drives within a biological network affect gene transcription.

Here, we consider a simple, yet generic, framework for the solution of the ME of gene transcription and degradation for single cells under upstream drives, i.e., when the transcription and degradation parameters are time-dependent functions or stochastic variables. We show that the exact solution  $P(n, t)$  for such a model naturally decouples into two parts: a discrete transcriptional Poissonian downstream component, which is common to all transcription models of this kind, and a model-specific continuous component, which describes the dynamics of the parameters reflecting the upstream variation. To obtain the full solution  $P(n, t)$  one only needs to calculate the probability density for the model-specific upstream drive, which we show corresponds to a continuous variable satisfying a linear random differential equation directly related to traditional differential rate equations of chemical kinetics. Our results can thus be thought of as a generalisation of the Poisson representation [17, 16] (originally defined as an *ansatz* with constant rate parameters) to allow for both time-varying and stochastic rates in transcription-degradation systems. Our work also departs from the work of Jahnke and Huisinga [24] by allowing the presence of cell-to-cell variability (or uncertainty) in the dynamical drive.

Below, we present the full properties of the general solution, and we derive the relationship of the observable time-varying moments with the moments of the dynamic upstream component. Because our framework treats dynamic and population variability consistently, we clarify the different effects of vari-

ability in the drives by considering the Fano factor across the population and across time. To illustrate the utility of our approach, we present analytical and numerical analyses of several models from the literature, which are shown to simply correspond to different upstream drives, deterministic or stochastic. These examples highlight our modelling approach: a flexible solvable model with upstream dynamic variability, reflecting the generic hypothesis that experimentally observed outputs are usually driven by fluctuating, usually unmeasurable and uncertain, upstream intra- and extra-cellular signals. Our framework provides a means to characterise such upstream variability, dynamical and population-wide, and we provide examples of its use for computational biology and data analysis in relation to experiments.

## 2 The master equation for gene transcription in populations of cells with upstream drives

### Notation and formulation of the problem

To study gene expression in a single cell with time-dependent upstream drives, we consider the stochastic process in continuous time  $t$ ,  $N = \{N_t \in \mathbb{N} : t \geq 0\}$ , where  $N_t$  is a discrete random variable describing the number of mRNA molecules in the cell. We look to obtain the probability mass function,  $P(n, t) := \Pr(N_t = n)$ .

The mRNA copy number increases via transcription events and decreases via degradation events but, importantly, we acknowledge that the observed gene reflects the dynamic variability of intra- and extra-cellular processes and that cells are heterogeneous. Thus, the transcription and degradation rates can depend on time and can be different for each cell (Fig. 1). To account for such variability, we describe transcription and degradation rates as stochastic processes  $M = \{M_t \in \mathbb{R}^+ : t \geq 0\}$  and  $L = \{L_t \in \mathbb{R}^+ : t \geq 0\}$ , without specifying any functional form except requiring that  $M$  and  $L$  do not depend on the number of mRNA molecules already present. Deterministic time-varying transcription/degradation rates, with or without cell-to-cell correlations, are a particular case of this definition.

Following standard notation in the stochastic processes literature,  $M_t$  and  $L_t$  denote the random variables at time  $t$ . To simplify notation, however, we depart from standard notation and denote the sample paths (i.e., realisations) of  $M$  and  $L$  by  $\{\mu(t)\}_{t \geq 0}$  and  $\{\lambda(t)\}_{t \geq 0}$ , respectively, thinking of them as particular functions of time describing the transcription and degradation rates under the changing cellular state and environmental conditions in an ‘example’ cell (Fig. 1). The sample paths of other random variables are denoted similarly, e.g., the sample paths of  $N_t$  are  $\{\nu(t)\}_{t \geq 0}$ .

The sample paths  $\{\mu(t)\}_{t \geq 0}$  and  $\{\lambda(t)\}_{t \geq 0}$  represent *cellular drives* encapsulating the variability across time and across the population consistently. This formulation unifies several models in the literature, which implicitly or explicitly assume time-varying transcription and/or degradation processes [43, 45, 21, 49, 55, 52, 77], and can be shown to correspond to particular types of dynamic upstream variability. In addition, the framework allows us to specify cell-to-cell correlations across the population, which we refer to as the ‘degree of synchrony’. A population will be *perfectly synchronous* when the sample paths of the drives for every cell in the population are identical, i.e., if  $M_t$  and  $L_t$  have zero variance. If, however, transcription and/or degradation rates differ between cells,  $M_t$  and  $L_t$  themselves emerge from a probability density: the wider the density, the more asynchronous the cellular drives are (Fig. 1).

Our aim is to obtain the probability distribution of the copy number  $N_t$  under upstream time-varying

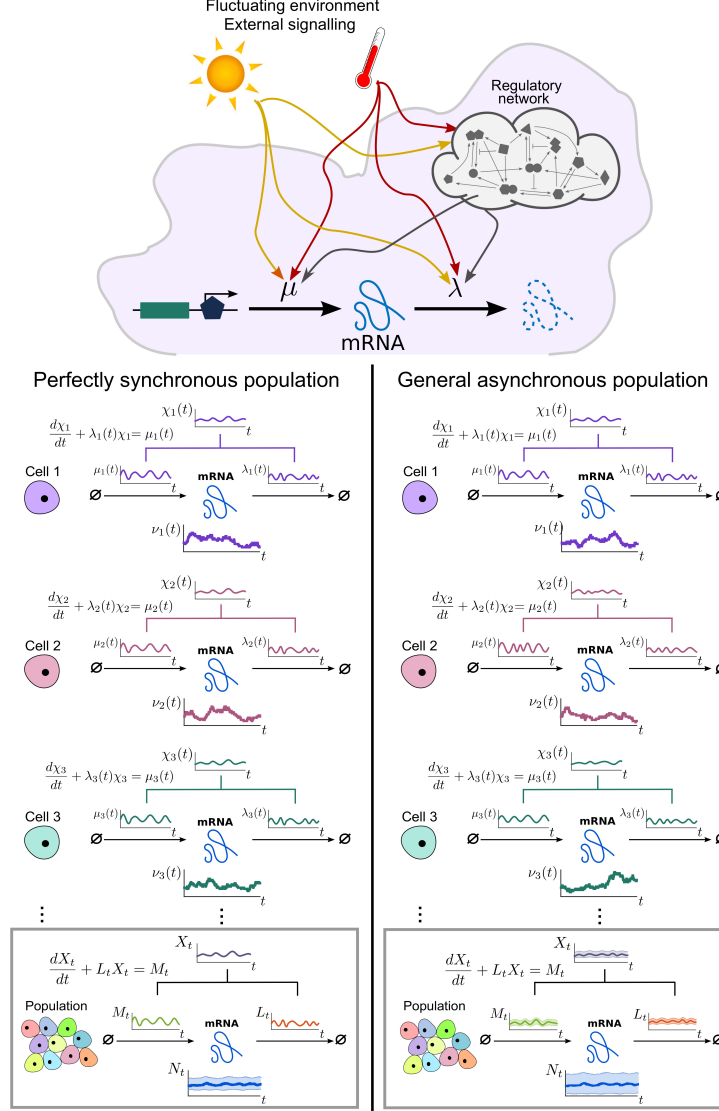


Figure 1: Single-cell gene transcription under upstream drives. The transcription of each cell  $i$  takes place under particular cellular drives  $\{\mu_i(t)\}_{t \geq 0}$  and  $\{\lambda_i(t)\}_{t \geq 0}$ , representing time-varying transcription and degradation rates. Both cellular drives are combined into the upstream effective drive  $\{\chi_i(t)\}_{t \geq 0}$ , which dictates the long-term probability distribution describing the stochastic gene expression  $\{\nu_i(t)\}_{t \geq 0}$  within each cell (10). When there is cell-to-cell variability in the population, the cellular drives are described by processes  $M$  and  $L$  leading to the upstream effective drive  $X$ . The probability distribution of the population corresponds to the mixture of the upstream process  $X$  and the Poissonian downstream transcriptional component, as given by (14). Increased synchrony in the population implies decreased ensemble variability of the random variables  $M_t$ ,  $L_t$ ,  $X_t$ , and  $N_t$ .

cellular drives  $M_t$  and  $L_t$ , themselves containing stochastic parameters reflecting cell-to-cell variability. We proceed in two steps: first, we obtain the solution for the perfectly synchronous system without cell-to-cell variability; then we consider the general asynchronous case.

## 2.1 Perfectly synchronous population

As a first step to the solution of the general case, consider a population of cells with perfectly synchronous transcription and degradation rate functions,  $M = \{\mu(t)\}_{t \geq 0}$  and  $L = \{\lambda(t)\}_{t \geq 0}$ ; i.e., the transcription and degradation processes are defined by the same sample path for the whole population and the stochastic processes  $M$  and  $L$  have zero variance at all times (Fig. 1).

In the perfectly synchronous case, we have an immigration-death process with reaction diagram:



and its ME is standard:

$$\begin{aligned} \frac{d}{dt} P(n, t | \{\mu(\tau)\}_{\tau \in [0, t]}, \{\lambda(\tau)\}_{\tau \in [0, t]}) &= \mu(t) P(n-1, t | \{\mu(\tau)\}_{\tau \in [0, t]}, \{\lambda(\tau)\}_{\tau \in [0, t]}) \\ &+ (n+1) \lambda(t) P(n+1, t | \{\mu(\tau)\}_{\tau \in [0, t]}, \{\lambda(\tau)\}_{\tau \in [0, t]}) - (\mu(t) + n \lambda(t)) P(n, t | \{\mu(\tau)\}_{\tau \in [0, t]}, \{\lambda(\tau)\}_{\tau \in [0, t]}), \end{aligned} \quad (2)$$

where  $P(n, t | \{\mu(\tau)\}_{\tau \in [0, t]}, \{\lambda(\tau)\}_{\tau \in [0, t]})$  denotes the probability of having  $n$  mRNAs at time  $t$  for the given history of the cellular drives  $\{\mu(\tau)\}_{\tau \in [0, t]}$  and  $\{\lambda(\tau)\}_{\tau \in [0, t]}$ .

Using the probability generating function

$$G(z, t) = \sum_{n=0}^{\infty} z^n P(n, t | \{\mu(\tau)\}_{\tau \in [0, t]}, \{\lambda(\tau)\}_{\tau \in [0, t]}),$$

we transform the ME (2) into

$$\frac{\partial G}{\partial t} = (z-1) \mu(t) G - (z-1) \lambda(t) \frac{\partial G}{\partial z}.$$

Without loss of generality, let us first consider an initial condition with  $n_0$  mRNA molecules. Using the method of characteristics, we obtain the solution:

$$G(z, t | n_0) = \left[ (z-1) e^{-\int_0^t \lambda(\tau) d\tau} + 1 \right]^{n_0} e^{\chi(t)(z-1)}, \quad (3)$$

which is given in terms of

$$\chi(t) := \int_0^t \mu(\tau) e^{-\int_{\tau}^t \lambda(\tau') d\tau'} d\tau. \quad (4)$$

We will refer to the time-varying continuous function  $\chi(t)$  as the *effective drive*, as it integrates the effect of both cellular drives.

Notice that the solution (3) can be rewritten as the product of two probability generating functions:

$$G(z, t|n_0) =: G_{\text{Bin}}(z, t|n_0) G_{\text{Poi}}(z, t),$$

corresponding to a binomial and a Poisson distribution, respectively. Hence, for the perfectly synchronous case, the solution is given by:

$$N_t = N_t^{ic}|n_0 + N_t^s, \quad \text{with} \quad (5)$$

$$N_t^{ic}|n_0 \sim \text{Bin}\left(n_0, e^{-\int_0^t \lambda(\tau) d\tau}\right) \quad (6)$$

$$N_t^s \sim \text{Poi}(\chi(t)), \quad (7)$$

where  $N_t^{ic}|n_0$  is a binomial random variable with  $n_0$  trials and success probability  $e^{-\int_0^t \lambda(\tau) d\tau}$ , and  $N_t^s$  is a Poisson random variable with parameter  $\chi(t)$ . The physical interpretation of this breakdown is that  $N_t^{ic}$  describes the mRNA transcripts that were initially present in the cell and still remain at time  $t$ , whereas  $N_t^s$  describes the number of mRNAs transcribed since  $t = 0$ .

Since  $N_t^{ic}$  and  $N_t^s$  are independent, it is easy to read off the first two moments directly:

$$\mathbb{E}[N_t|\{\mu(\tau)\}_{\tau \in [0, t]}, \{\lambda(\tau)\}_{\tau \in [0, t]}, n_0] = \mathbb{E}[N_t^{ic}|n_0] + \mathbb{E}[N_t^s] = n_0 e^{-\int_0^t \lambda(\tau) d\tau} + \chi(t);$$

$$\text{Var}(N_t|\{\mu(\tau)\}_{\tau \in [0, t]}, \{\lambda(\tau)\}_{\tau \in [0, t]}, n_0) = \text{Var}(N_t^{ic}|n_0) + \text{Var}(N_t^s) = n_0 e^{-\int_0^t \lambda(\tau) d\tau} \left(1 - e^{-\int_0^t \lambda(\tau) d\tau}\right) + \chi(t).$$

From (5)–(7), the full distribution is:

$$\begin{aligned} P(n, t|\{\mu(\tau)\}_{\tau \in [0, t]}, \{\lambda(\tau)\}_{\tau \in [0, t]}, n_0) &= \Pr(N_t^{ic} + N_t^s = n|n_0) = \sum_{k=0}^n \Pr(N_t^{ic} = k|n_0) \Pr(N_t^s = n - k) \\ &= \sum_{k=0}^n \binom{n_0}{k} \left(e^{-\int_0^t \lambda(\tau) d\tau}\right)^k \left(1 - e^{-\int_0^t \lambda(\tau) d\tau}\right)^{n_0-k} \frac{\chi(t)^{n-k}}{(n-k)!} e^{-\chi(t)}. \end{aligned} \quad (8)$$

This mathematical form is well-known when the rates are constant [66, 16], and a classical result in queueing theory [11]. We also remark that the solution with time-dependent rates (8) is the one-gene case of the main result in Jahnke and Huisinga [24].

If the initial state is itself described by a random variable  $N_0$  with its own probability distribution, we apply the law of total probability to obtain the solution in full generality as (see Appendix A):

$$\begin{aligned} P(n, t|\{\mu(\tau)\}_{\tau \in [0, t]}, \{\lambda(\tau)\}_{\tau \in [0, t]}) &= \sum_{n_0} P(n, t|\{\mu(\tau)\}_{\tau \in [0, t]}, \{\lambda(\tau)\}_{\tau \in [0, t]}, n_0) \Pr(N_0 = n_0) \\ &= \sum_{k=0}^n \Pr(N_t^s = n - k) \Pr(N_t^{ic} = k), \end{aligned} \quad (9)$$

where  $N_t^s$  is distributed according to (5)–(7), and  $\Pr(N_t^{ic} = k)$  is the mixture of the time-dependent binomial distribution (5) and the distribution of the initial condition  $N_0$ .

**The initial transient ‘burn in’ period.** For biologically realistic degradation rates  $\{\lambda(t)\}_{t \geq 0}$ , the contribution from the initial condition ( $N_t^{ic}$ ) decreases exponentially. Hence as time grows the transcripts present at  $t = 0$  degrade, and the population is expected to be composed of mRNAs transcribed after  $t = 0$ .

If the initial distribution of  $N_0$  is not the stationary distribution of the ME (or, more generally, not equal to the attracting distribution of the ME, as defined in Appendix A), there is an initial time-dependence of  $P(n, t)$  lasting over a time scale  $T^{ic}$  (given by  $\int_0^{T^{ic}} \lambda(\tau) d\tau \approx 1$ ), which corresponds to a ‘burn-in’ transient associated with the decay of the initial condition. We remark that the time-dependence described in Refs. [21, 54, 69, 58] corresponds only to this ‘burn-in’ transient (see also Fig. 7).

On the other hand, when the initial distribution of  $N_0$  is the stationary distribution (or the attracting distribution) of the ME, the component containing the initial condition ( $N_t^{ic}$ ) and the long-term component ( $N_t^s$ ) balance each other at every point in time, maintaining stationarity (or the attracting distribution), as shown analytically in Appendix A.

**The long-term behaviour of the solution.** In this work, we focus on the time dependence of  $P(n, t)$  induced through non-stationarity of the parameters and/or correlated behaviour of the cells within the population. Hence for the remainder of the paper, we neglect the transient terms. Consequently, for perfectly synchronous cellular drives, the solution of the ME (2) is a Poisson random variable with time-dependent rate equal to the effective upstream drive,  $\chi(t)$ :

$$[N_t | \chi(t)] \approx [N_t^s | \chi(t)] \sim \text{Poi}(\chi(t)),$$

with distribution

$$P(n, t | \{\mu(\tau)\}_{\tau \in [0, t]}, \{\lambda(\tau)\}_{\tau \in [0, t]}) = P(n, t | \chi(t)) = \frac{\chi(t)^n}{n!} e^{-\chi(t)}, \quad (10)$$

which makes explicit the dependence on the *history* of the sample paths  $\{\mu(\tau)\}_{\tau \in [0, t]}, \{\lambda(\tau)\}_{\tau \in [0, t]}$ , which is encapsulated in the *value* of the effective drive  $\chi(t)$  at time  $t$ .

Indeed, from (4) it follows that the sample path  $\{\chi(t)\}_{t \geq 0}$  satisfies a first order linear ordinary differential equation with time-varying coefficients:

$$\frac{d\chi}{dt} + \lambda(t) \chi = \mu(t), \quad (11)$$

which is the rate law for a chemical reaction with zeroth-order production with rate  $\mu(t)$ , and first-order degradation with rate  $\lambda(t)$  per mRNA molecule. For biologically realistic (i.e., positive and finite) cellular drives,  $\chi(t)$  is a continuous function.

## 2.2 The general asynchronous case: cell-to-cell variability in the cellular drives

Consider now the general case where different sample paths for the cellular drives are possible, i.e., we allow explicitly for the transcription and degradation rates to vary from cell to cell. The cell population will have some degree of asynchrony, hence  $M_t$  and  $L_t$  have non-zero variance for at least some  $t \geq 0$ . The transcription and degradation rates are then described by stochastic processes  $M$  and  $L$ :



and the collection of all differential equations of the form (11) is represented formally by the random differential equation<sup>1</sup>

$$\frac{dX_t}{dt} + L_t X_t = M_t. \quad (13)$$

Equations of this form appear in many sciences, and a large body of classical results allows us to determine the probability density function of the upstream process,  $X_t$  [68, 59, 41]. Below, we use such results to obtain  $f_{X_t}(x, t)$  for biologically relevant models.

Note that from Eq. (10) and the law of total probability, it follows that the probability mass function for the random variable  $N_t$  under cellular drives described by the random processes  $M$  and  $L$  is given by the *Poisson mixture* (or compound) distribution:

$$P(n, t) = P_{X_t}(n, t) = \int \frac{x^n}{n!} e^{-x} f_{X_t}(x, t) dx, \quad (14)$$

where the density  $f_{X_t}(x, t)$  of the effective drive  $X_t$  (to be determined) can be understood as a *mixing density*. The notation  $P_{X_t}(n, t)$  recalls explicitly the dependence of the solution on the density of  $X_t$ , but we drop this reference and use  $P(n, t)$  below to simplify notation. The problem of solving the full ME is thus reduced to finding the mixing density  $f_{X_t}(x, t)$ . Note that for synchronous drives, we have  $f_{X_t}(x, t) = \delta(\chi(t) - x)$ , where  $\delta$  is the Dirac delta function, and (14) reduces to (10).

Equation (14) also shows that there are two separate sources of variability in gene expression, contributing to the distribution of  $N_t$ . One source of variability is the Poisson nature of transcription and degradation, common to every model of the form considered here; the second source is the time-variation or uncertainty in the cellular drives, encapsulated in the upstream process  $X_t$  describing the ‘degree of synchrony’ between cells and/or their variability over time. In this sense, Eq. (14) connects with the concept of separable ‘intrinsic’ and ‘extrinsic’ components of gene expression noise pioneered by Swain *et al.* [12, 63, 19, 5]. Yet rather than considering moments, the full distribution  $P(n, t)$  is separable into a model-dependent ‘upstream component’ given by  $f_{X_t}(x, t)$ , and a downstream transcriptional ‘Poisson component’ common to all models of this type.

### 3 The effective upstream drive in gene transcription models

The generic model of gene transcription and degradation with time-dependent drives introduced above provides a unifying framework for several models previously considered in isolation. In this section, we exemplify the tools to obtain the density of the effective drive  $f_{X_t}(x, t)$  analytically or numerically through relevant examples.

#### 3.1 Gene transcription under upstream drives with static randomness

In this first section, we consider models of gene transcription where the upstream drives are deterministic, yet with random parameters representing cell variability.

---

<sup>1</sup>We do not use the term *stochastic* differential equation (SDE), because SDEs are usually associated with random white noise.

### 3.1.1 Random entrainment to upstream sinusoidal drives: random phase offset in transcription or degradation rates

Equation (13) can sometimes be solved directly to obtain  $f_{X_t}(x, t)$  from a transformation of the random variables  $M_t$  and  $L_t$ . We now show two such examples, where we explore the effect of entrainment of gene transcription and degradation to an upstream periodic drive [31].

First, consider a model of gene transcription of the form (12) with transcription rate given by a sinusoidal function and where each cell has a random phase. This *random entrainment* (RE) model is a simple representation of a cell population with transcription entrained to an upstream rhythmic signal, yet with a random phase offset for each cell:

$$\begin{aligned} M_t &:= m \frac{1 + \cos(\omega t + \Phi)}{2} \\ L_t &:= 1. \end{aligned} \tag{15}$$

Here  $m$  and  $\omega$  are given constants and  $\Phi$  is a (static) random variable describing cell-to-cell variability (or uncertainty). Solving Eq. (13) in this case, we obtain

$$\begin{aligned} X_t &= \frac{m(1 + \omega^2 + \cos(\omega t + \Phi) + \omega \sin(\omega t + \Phi))}{2(1 + \omega^2)} \\ &= B + A \sin(\omega t + \Phi^*), \end{aligned}$$

where  $A = m/2\sqrt{1 + \omega^2}$ ,  $B = m/2$  and  $\Phi^* = \Phi + \arctan(1/\omega)$ .

Suppose  $\Phi^*$  is uniformly distributed on  $[-r, r]$ ,  $r \leq \pi$ . Inverting the sine with  $\Phi^*$  restricted to  $[-r, r]$ , we obtain

$$f_{X_t}(x, t) = \frac{k(t)}{2r\sqrt{A^2 - (x - B)^2}}, \tag{16}$$

where  $k(t) \in \{0, 1, 2\}$  is the number of solutions of  $\sin \theta = (x - B)/A$  for  $\theta \in (\omega t - r, \omega t + r)$ . As the phase distribution of the drives becomes narrower, the upstream variability disappears:  $r \rightarrow 0 \implies f_{X_t}(x, t) \rightarrow \delta((B + A \sin \omega t) - x)$ . In this limit, all cells follow the entraining drive exactly, and  $P(n, t)$  becomes a Poisson distribution at all times.

Figure 2 depicts  $f_{X_t}$  for  $r = 0$  (no cell-to-cell phase variation, (a)) and for  $r = \pi/2$ , and  $r = \pi$  (increasingly wider uniform distribution of phases, (b) and (c)). The full distribution  $P(n, t)$  is obtained using (16) and (14).

Second, let us consider the same model of entrainment to an upstream sinusoidal signal with a random offset, but this time via the degradation rate:

$$\begin{aligned} M_t &:= m, \\ L_t &:= b + a \cos(\omega t + \Phi), \end{aligned} \tag{17}$$

with  $m$ ,  $a$ ,  $b$ , and  $\omega$  given constants, and  $\Phi$  a (static) random variable.

Eq. (13) can be solved approximately [31] to give

$$X_t = B + A \sin(\omega t + \Phi^*),$$

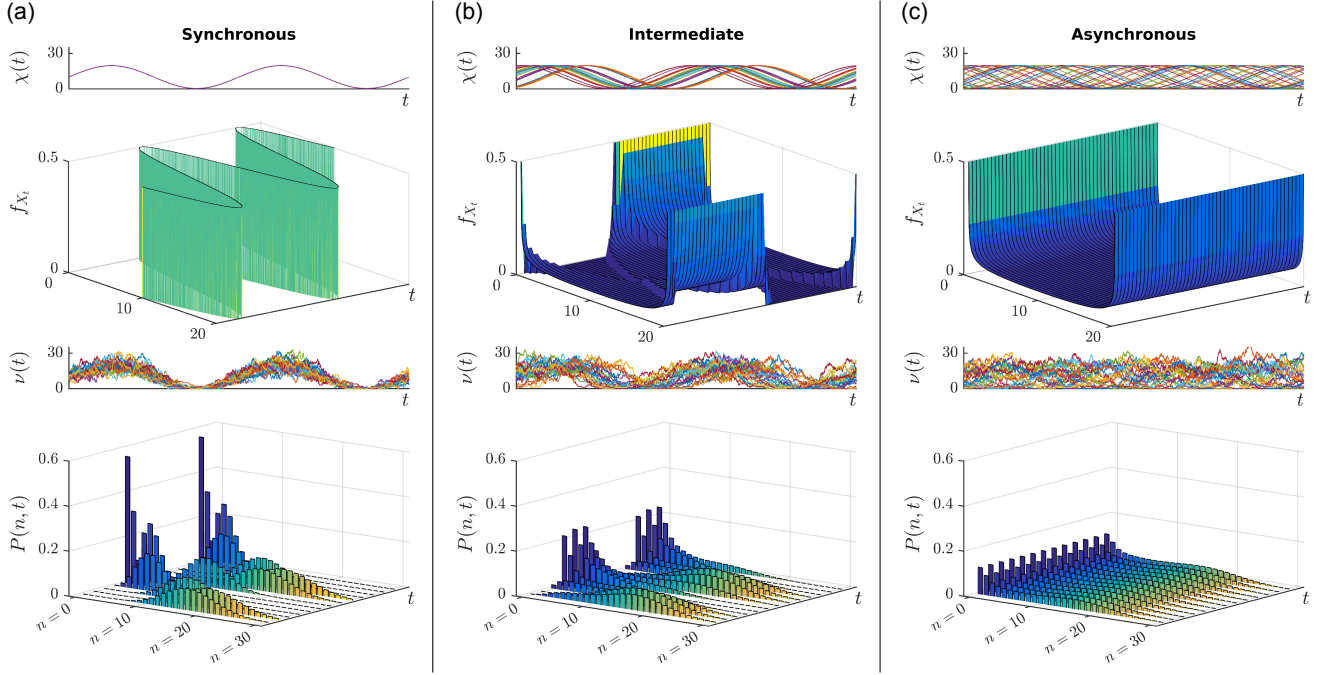


Figure 2: Gene transcription under the random entrainment model (15) with constant degradation rate and transcription rates entrained to an upstream sinusoidal signal with  $\omega = 1$ . Each cell has a random phase offset  $\phi$  drawn from a distribution. (a) The synchronous population corresponds to identical phases across the population. In this case, the transcription reflects the time variability of the upstream drive mixed with the stochasticity due to the downstream Poisson process of transcription. When the random phases  $\phi$  are uniformly distributed on an interval of range (b)  $\pi$  and (c)  $2\pi$ , the population becomes increasingly asynchronous. For all three cases, we show (top to bottom): sample paths of the effective drive,  $X$ ; its density  $f_{X_t}(x, t)$  given by Eq. (16); sample paths of the number of mRNAs,  $N$ ; and the full solution of the ME  $P(n, t)$ .

where  $A = 2ma\sqrt{1 + (\omega/b)^2}/[2(b^2 + \omega^2) - a^2]$ ,  $B = Ab\sqrt{1 + (\omega/b)^2}/a$ , and  $\Phi^* = \Phi + \pi + \arctan(b/\omega)$ . As before, if  $\Phi^*$  is uniform on  $[-r, r]$ ,  $r \leq \pi$ , the density of the effective drive takes the same form (16) as above.

### 3.1.2 Upstream Kuramoto promoters with varying degree of synchronisation

As an illustrative computational example, we study a population of cells whose promoter strengths display a degree of synchronisation across the population. To model this upstream synchronisation, consider the *Kuramoto promoter model*, where the promoter strength of each cell  $i$  depends on an oscillatory phase  $\theta_i(t)$ ,

and cells are coupled via a Kuramoto model [29, 60, 23]. We then have a model of the form (12) with:

$$\begin{aligned} M_t &:= m \frac{b + \cos(\Theta(t; \Omega))}{2} \\ L_t &:= 1. \end{aligned} \tag{18}$$

Here  $m, b$  are constants and  $\{\theta_i(t)\}_{i=1}^C$  are the phase variables for the  $C$  cells governed by the globally coupled Kuramoto model:

$$\frac{d\theta_i}{dt} = \omega_i + \frac{K}{C} \sum_{j=1}^C \sin(\theta_j - \theta_i), \tag{19}$$

where  $K$  is the coupling parameter and the intrinsic frequency of each cell,  $\omega_i$ , is drawn from the random distribution  $\Omega \sim \mathcal{N}(0, 0.05^2)$ . The Kuramoto model allows us to tune the degree of synchrony through the coupling  $K$ : for small  $K$ , the cells do not display synchrony since they all have a slightly different intrinsic frequency; as  $K$  is increased, the population becomes more synchronised.

This model is a simple representation of nonlinear synchronisation processes in cell populations with intrinsic heterogeneity [15, 64, 36, 67]. In Figure 6(a), we show how the sample paths change as the degree of synchrony increases, and we exemplify the use of (14) for the numerical solution of the gene expression of this model.

### 3.2 Asynchronous transcription under stochastic multistate promoters

In the previous section, we obtained  $f_{X_t}(x, t)$  by capitalising on the precise knowledge of the sample paths of  $M$  and  $L$  to solve (13) explicitly. In other cases, we can obtain  $f_{X_t}(x, t)$  by following the usual procedure of writing down an evolution equation for the probability density of an *expanded* state that is Markovian, and then marginalising. More specifically, let the vector process  $\mathbf{Y}$  prescribe the upstream drives, so that  $M = M(\mathbf{Y}, t)$  and  $L = L(\mathbf{Y}, t)$ , and consider the expanded state  $\mathbf{X}_t := (X_t, \mathbf{Y}_t)$ . Note that since  $\mathbf{Y}$  is upstream, it prescribes  $X$  (and not vice versa). We can then write the evolution equation for the joint probability density  $f_{\mathbf{X}_t}(x, \mathbf{y}, t)$ :

$$\frac{\partial}{\partial t} f_{\mathbf{X}_t}(x, \mathbf{y}, t) = - \frac{\partial}{\partial x} [(\mu(\mathbf{y}, t) - \lambda(\mathbf{y}, t)x) f_{\mathbf{X}_t}(x, \mathbf{y}, t)] + \mathcal{L}_{\mathbf{Y}_t} [f_{\mathbf{X}_t}(x, \mathbf{y}, t)], \tag{20}$$

which follows from conservation of probability. In Equation (20), the differential operator for  $X$ , which follows from (13), is the first jump moment [42] conditional upon  $\mathbf{Y}_t = \mathbf{y}$  (and hence upon  $M_t = \mu(\mathbf{y}, t)$  and  $L_t = \lambda(\mathbf{y}, t)$ ); the second term  $\mathcal{L}_{\mathbf{Y}_t}[\cdot]$  is the infinitesimal generator of the upstream processes. In particular, for continuous stochastic processes  $\mathcal{L}_{\mathbf{Y}_t}[\cdot]$  is of Fokker-Planck type, and for Markov chains  $\mathcal{L}_{\mathbf{Y}_t}[\cdot]$  is a transition rate matrix. The desired density  $f_{X_t}(x, t)$  can then be obtained via marginalisation.

Equation (20) can be employed to analyse the widely used class of transcription models with asynchronous, random promoter switching between discrete states, where each state has different transcription and degradation rates representing different levels of promoter activity due to, e.g., transcription factor binding or chromatin remodelling [49]. A classic example is the *random telegraph* (RT) model, first used by Ko in 1991 [26] to explain cell-to-cell heterogeneity and bursty transcription (Fig. 3a).

In our framework, such random promoter switching can be understood as an upstream *stochastic* process driving transcription as follows. Let us assume that the promoter can attain  $D$  states  $s$ , and each state has

constant transcription rate  $m_s$  and constant degradation rate  $\ell_s$ . The state of the promoter is described by a random process  $S = \{S_t \in \{1, 2, \dots, D\} : t \geq 0\}$ , with sample paths denoted by  $\{\varsigma(t)\}_{t \geq 0}$ , and its evolution is governed by the  $D$ -state Markov chain with transition rate  $k_{sr}$  from state  $r$  to state  $s$ . The state of the promoter  $S_t = s$  prescribes that  $M_t = m_s$  and  $L_t = \ell_s$ . Hence, the sample paths of  $M$  and  $L$  are a succession of step functions with heights  $m_s$  and  $\ell_s$ , respectively, occurring at exponentially distributed random times.

As described above, we expand the state space of the cellular drives to include the promoter state  $\mathbf{X}_t = \{X_t, S_t\}$ . The evolution equation (20) is then given by  $D$  coupled equations:

$$\frac{\partial}{\partial t} f_{X_t, S_t}(x, s, t) = -\frac{\partial}{\partial x} [(\mu_s - \lambda_s x) f_{X_t, S_t}(x, s, t)] + \sum_{j=1}^D k_{sj} f_{X_t, S_t}(x, j, t) - \sum_{j=1}^D k_{js} f_{X_t, S_t}(x, s, t),$$

$$s = 1, 2, \dots, D, \quad (21)$$

which can be thought of as a set of multistate Fokker-Planck-Kolmogorov equations [42]. Marginalisation then leads to the density of the effective drive:

$$f_{X_t}(x, t) = \sum_{s=1}^D f_{X_t, S_t}(x, s, t), \quad (22)$$

and the full ME solution is obtained from (22) and (14).

We illustrate this approach more explicitly with two examples (Fig. 3): a re-derivation of the known solution of the standard RT model; and the solution of the 3-state cyclic model with a refractory state. Results for other promoter architectures are discussed in [10].

### 3.2.1 The Random Telegraph model (2 states)

Although the RT model has been solved by several methods [43, 45, 21], we briefly rederive its solution within the above framework to clarify its generalisation to other promoter architectures.

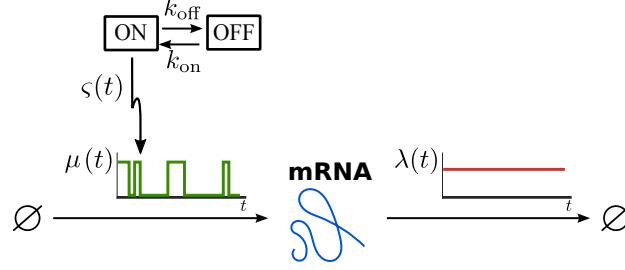
Consider the standard RT model (Fig. 3a), with promoter switching stochastically between the active state  $s_{\text{on}} = 1$ , with constant transcription rate  $m_1 = m$ , and the inactive state  $s_{\text{off}} = 0$ , where no transcription takes place,  $m_0 = 0$ . The transition rates between the two states are  $k_{10} = k_{\text{on}}$  and  $k_{01} = k_{\text{off}}$ . Without loss of generality, we assume  $\ell_1 = \ell_0 = \lambda(t) \equiv 1$ . The transcription model is of the form (12) with:

$$\begin{aligned} M_t &:= m S_t \\ L_t &:= 1, \end{aligned} \quad (23)$$

where  $S = \{S_t \in \{0, 1\} : t \geq 0\}$  with waiting times drawn from exponential distributions:  $\tau_{\text{off}} \sim \exp(1/k_{\text{on}})$  and  $\tau_{\text{on}} \sim \exp(1/k_{\text{off}})$ .

Let  $Z_t = X_t/m$ , and denote  $f_{\text{on}}(z, t) := f_{Z_t, S_t}(z, s_{\text{on}}, t)$  and  $f_{\text{off}}(z, t) := f_{Z_t, S_t}(z, s_{\text{off}}, t)$ , with  $z \in (0, 1)$ .

(a) Random telegraph model (2 states)



(b) Refractory promoter model (3 states)

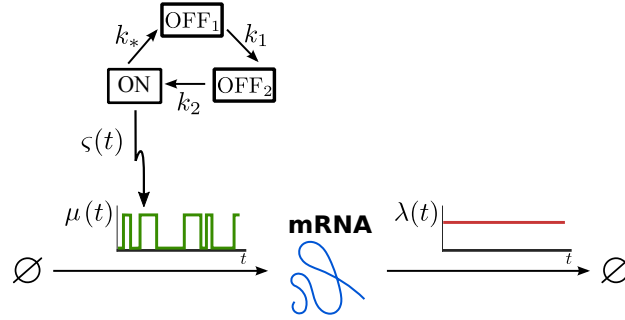


Figure 3: Asynchronous stochastic promoter switching models correspond to upstream stochastic processes. The promoter cycles between the discrete states, transitioning stochastically with rates as indicated: (a) the standard 2-state random telegraph (RT) model; (b) the 3-state refractory promoter model.

Then the multistate Fokker-Planck-Kolmogorov equations (21) are:

$$\begin{aligned} \frac{\partial f_{\text{on}}}{\partial t} &= -\frac{\partial}{\partial z} [(1-z)f_{\text{on}}] - k_{\text{off}}f_{\text{on}} + k_{\text{on}}f_{\text{off}} \\ \frac{\partial f_{\text{off}}}{\partial t} &= -\frac{\partial}{\partial z} [-zf_{\text{off}}] + k_{\text{off}}f_{\text{on}} - k_{\text{on}}f_{\text{off}}, \\ f_{Z_t} &= f_{\text{on}} + f_{\text{off}} \end{aligned}$$

with integral conditions  $\int_0^1 f_{\text{on}}(z, t) dz = P(S_t = s_{\text{on}})$  and  $\int_0^1 f_{\text{off}}(z, t) dz = P(S_t = s_{\text{off}})$ .

At stationarity, it then follows [57] that

$$f_{Z_t}(z) = \frac{z^{k_{\text{on}}-1}(1-z)^{k_{\text{off}}-1}}{\text{B}(k_{\text{on}}, k_{\text{off}})}, \quad (24)$$

where  $\text{B}(a, b) = \Gamma(a)\Gamma(b)/\Gamma(a+b)$  is the Beta function. In other words, at stationarity, the normalised effective drive is described by a Beta distribution:

$$Z_t \sim \text{Beta}(k_{\text{on}}, k_{\text{off}}), \quad \forall t.$$

Using (24) and (14), we obtain that the full stationary solution is the Poisson-Beta mixture:

$$\begin{aligned} P(n) &= \int_0^1 \frac{(mz)^n}{n!} e^{-mz} \frac{z^{k_{\text{on}}-1}(1-z)^{k_{\text{off}}-1}}{\text{B}(k_{\text{on}}, k_{\text{off}})} dz \\ &= \frac{\Gamma(k_{\text{on}} + n)}{\Gamma(k_{\text{on}})} \frac{\Gamma(k_{\text{on}} + k_{\text{off}})}{\Gamma(k_{\text{on}} + k_{\text{off}} + n)} \frac{m^n}{\Gamma(n+1)} {}_1F_1(k_{\text{on}} + n, k_{\text{on}} + k_{\text{off}} + n; -m), \end{aligned} \quad (25)$$

where  ${}_1F_1(a, b; z)$  is the confluent hypergeometric function [1].

### 3.2.2 The Refractory Promoter model (3 states)

In the standard RT model, the waiting times in each state are exponentially distributed. In recent years, time course data have shown that the  $\tau_{\text{off}}$  do not conform to an exponential distribution, leading some authors to incorporate a second inactive (refractory) state, which needs to be cycled through before returning to the active state [62, 77]. The net ‘OFF’ time is then the sum of two exponentially distributed waiting times.

In this *refractory promoter model* (Fig. 3b), the promoter switches through the states  $s_*$ ,  $s_1$ , and  $s_2$  with rates  $k_*$ ,  $k_1$  and  $k_2$ . Transcription takes place at constant rate  $m$  only when the promoter is in the active state  $s_*$  and, without loss of generality, we assume a constant degradation rate  $\lambda(t) \equiv 1$  for all states. This model is of the same form as (23), and is solved similarly.

Making the change of variables  $Z_t = \lambda X_t / m = X_t / m$  and, using the notation  $f_i(z, t) := f_{Z_t, S_t}(z, t, s_i)$ , the multistate Fokker-Planck-Kolmogorov equations are

$$\begin{aligned} \frac{\partial f_*}{\partial t} &= -\frac{\partial}{\partial z} [(1-z)f_*] - k_* f_* + k_2 f_2 \\ \frac{\partial f_1}{\partial t} &= -\frac{\partial}{\partial z} [-zf_1] + k_* f_* - k_1 f_1 \\ \frac{\partial f_2}{\partial t} &= -\frac{\partial}{\partial z} [-zf_2] + k_1 f_1 - k_2 f_2, \\ f_{Z_t} &= f_* + f_1 + f_2. \end{aligned}$$

with three integral conditions  $\int_0^1 f_i(z) dz = P(S = s_i)$ .

At stationarity, we find

$$\begin{aligned} f_{Z_t}(z) &= C_1 z^{k_1-1} {}_2F_1 \left[ a_+^{(1)}, a_-^{(1)}; 1 + k_1 - k_2; z \right] + C_2 z^{k_2-1} {}_2F_1 \left[ a_+^{(2)}, a_-^{(2)}; 1 - k_1 + k_2; z \right], \\ a_{\pm}^{(1)} &:= \frac{1}{2} (2 + k_1 - k_2 - k_* \pm d), \quad a_{\pm}^{(2)} := \frac{1}{2} (2 - k_1 + k_2 - k_* \pm d), \end{aligned}$$

where  $\{k_*, (k_1 - k_2), d := \sqrt{(k_* - k_1 - k_2)^2 - 4k_1 k_2}\} \notin \mathbb{Z}$  and  ${}_2F_1(a, b; c; z)$  is the Gauss hypergeometric function [1]. The full stationary solution  $P(n)$  is then obtained from (14).

For a detailed derivation (including expressions for the integration constants  $C_1$  and  $C_2$ ), see Appendix B.

### 3.3 Asynchronous multistate models with upstream promoter modulation

Finally, we consider a model of gene transcription that incorporates features of models described in Sections 3.1 and 3.2. Such a situation is of biological interest and appears when individual cells exhibit correlated dynamics in response to upstream factors (e.g., changing environmental conditions, drives or stimulations), but still maintain asynchrony in internal processes, such as transcription factor binding [74, 18].

To illustrate this concept, we consider the *modulated random telegraph* (MRT) model, a combination of the RE model (15) and the RT model (23), i.e., the promoter strength is modulated by an upstream sinusoidal drive with random phase  $\Phi$ , as in the RE model, yet the promoter switches stochastically between active/inactive states with rates  $k_{\text{on}}$  and  $k_{\text{off}}$ , as in the RT model. In this model, the transcription rate is correlated between cells through the entrainment to the upstream sinusoidal drive as a simple model for, e.g., circadian gene expression:

$$M_t := R_t(\Phi) S_t = m \frac{1 + \cos(\omega t + \Phi)}{2} S_t$$

$$L_t := 1,$$

where  $m, \omega > 0$  are constants;  $\Phi$  is the random phase across the cell population; and  $S = \{S_t \in \{0, 1\} : t \geq 0\}$ , with exponential waiting times, describes the stochastic promoter switching (Fig. 4a).

The solution of this model follows from the RT probability density (24) conditioned on the random phase  $\Phi$ , which prescribes the sample path  $\{\rho(t; \phi)\}_{t \geq 0}$  of the promoter strength  $R$ . The resulting scaled Beta distribution

$$f_{X_t|\Phi}(x, t|\phi) = \frac{x^{k_{\text{on}}-1} (\rho(t; \phi) - x)^{k_{\text{off}}-1}}{\text{B}(k_{\text{on}}, k_{\text{off}}) \rho(t; \phi)^{k_{\text{on}}+k_{\text{off}}-1}}$$

is then marginalised over the phase  $\Phi$  to obtain the density  $f_{X_t}(x, t)$  of the effective drive. For instance, if the phases are normally distributed  $\Phi \sim \mathcal{N}(0, \sigma^2)$ , we have (see Fig. 4b):

$$f_{X_t}(x, t) = \int f_{X_t|\Phi}(x, t|\phi) f_{\Phi}(\phi) d\phi = \int_{-\infty}^{\infty} \frac{x^{k_{\text{on}}-1}}{\text{B}(k_{\text{on}}, k_{\text{off}})} \frac{\left(\frac{m}{2}[1 + \cos(\omega t + \phi)] - x\right)^{k_{\text{off}}-1}}{\left(\frac{m}{2}[1 + \cos(\omega t + \phi)]\right)^{k_{\text{on}}+k_{\text{off}}-1}} \frac{e^{-\phi^2/2\sigma}}{\sigma\sqrt{2\pi}} d\phi.$$

As  $\sigma \rightarrow \infty$ , the population becomes asynchronous in the promoter strength, as well as in the state transitions, and time dependence wanes (Fig. 4b).

## 4 Ensemble noise characteristics in time-varying populations

In the previous sections, we were concerned with the full time-dependent probability distribution  $P(n, t)$  for the mRNA copy number  $N$ . However, in many circumstances such detailed information is not required, and simpler characterisations based on ensemble averages (e.g., Fano factor, coefficient of variation) are of interest. Simple corollaries from the Poisson mixture expression (14) allow us to derive expressions for the ensemble moments and other noise characteristics, as shown below. We remark that, in this section, all the expectations are taken over the distribution describing the cell population.

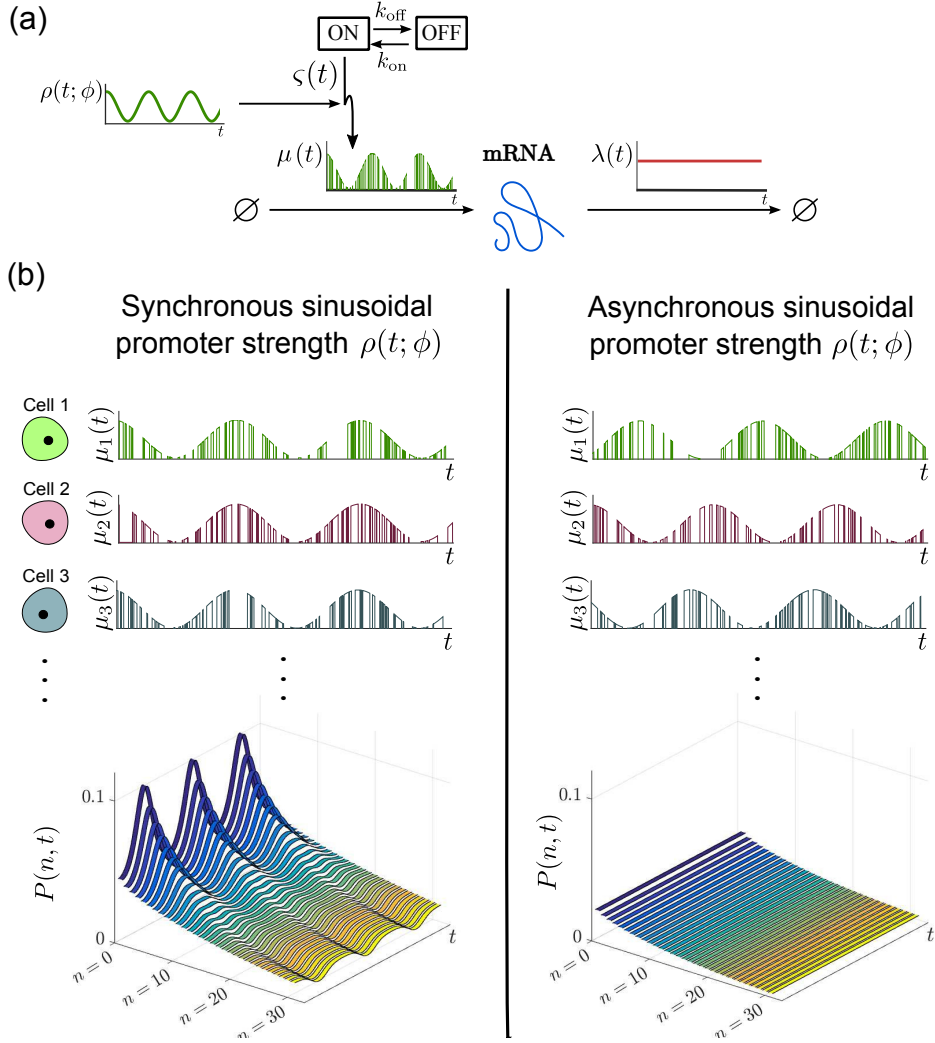


Figure 4: (a) Modulated Random Telegraph (MRT) model: each cell switches asynchronously between ‘ON’ and ‘OFF’ states, but the magnitude of the ‘ON’ transcription rate is modulated by the function  $\rho(t; \phi)$ , a sinusoid representing an upstream periodic process. The phase  $\phi$  represents the cell-to-cell variability and leads to the varying degree of synchrony across the population. (b) Sample paths  $\mu_i(t)$  and solution of the probability distribution  $P(n, t)$  of the MRT model for synchronous (left) and asynchronous (right) modulation. In the asynchronous case, the upstream drive has a random phase across the cells with distribution  $\Phi \sim \mathcal{N}(0, 10)$ .

#### 4.1 Time-dependent ensemble moments over the distribution of cells

To quantify noise characteristics of gene expression in a population, the ensemble moments  $\mathbb{E}[N_t^k]$ ,  $k \in \mathbb{N}$ ,  $t \geq 0$  are often determined via the probability generating function [43, 39, 76] or by integrating the master equation [51, 49, 50]. However, stationarity is usually assumed and the moments derived are not

suitable for time-varying systems. Here we use corollaries of the Poisson mixture expression (14) to derive expressions for the ensemble moments for time-varying systems under upstream drives.

From (10) we have  $[N_t|X_t = x] \sim \text{Poi}(x)$ ; hence

$$\mathbb{E}[N_t^k|X_t = x] = \sum_{r=1}^k x^r S(k, r), \quad \text{where} \quad S(k, r) = \sum_{j=0}^r \binom{r}{j} \frac{(-1)^{r-j} j^k}{r!}$$

are the Stirling numbers of the second kind [48]. The law of total probability then gives

$$\mathbb{E}[N_t^k] = \sum_{r=1}^k S(k, r) \mathbb{E}[X_t^r], \quad (26)$$

or, equivalently,

$$\begin{pmatrix} \mathbb{E}[N_t] \\ \mathbb{E}[N_t^2] \\ \vdots \\ \mathbb{E}[N_t^k] \end{pmatrix} = \begin{pmatrix} S(1, 1) & 0 & \dots & 0 \\ S(2, 1) & S(2, 2) & \dots & 0 \\ \vdots & \vdots & \ddots & \vdots \\ S(k, 1) & S(k, 2) & \dots & S(k, k) \end{pmatrix} \begin{pmatrix} \mathbb{E}[X_t] \\ \mathbb{E}[X_t^2] \\ \vdots \\ \mathbb{E}[X_t^k] \end{pmatrix}.$$

Therefore the ensemble moments of the mRNA copy number  $\mathbb{E}[N_t^k]$  can be obtained in terms of the moments of the effective drive  $\mathbb{E}[X_t^k]$ , and vice versa. For instance, it follows easily that  $\mathbb{E}[X_t] = \mathbb{E}[N_t]$ ;  $\text{Var}(X_t) = \text{Var}(N_t) - \mathbb{E}[N_t]$ ; and the skewness  $\gamma_1(X_t) = (\mathbb{E}[N_t^3] - 3\text{Var}(N_t) - 3\mathbb{E}[N_t]\text{Var}(N_t) - \mathbb{E}[N_t]^3)/(\text{Var}(N_t) - \mathbb{E}[N_t])^{3/2}$ .

**Decomposing the sources of noise:** From Eq. (26), it follows that the variability of the mRNA count  $N_t$  can be rewritten as:

$$\eta_N^2(t) := \frac{\text{Var}(N_t)}{(\mathbb{E}[N_t])^2} = \frac{1}{\mathbb{E}[N_t]} + \frac{\text{Var}(X_t)}{(\mathbb{E}[X_t])^2} = \eta_{\text{Poi}}^2(t) + \eta_{\text{up}}^2(t), \quad (27)$$

i.e., it can be decomposed into a Poissonian (downstream) component  $\eta_{\text{Poi}}^2(t)$  and an upstream component  $\eta_{\text{up}}^2(t)$  linked to the variable  $X_t$ . Note, however, that our expressions (26) provide decompositions for all moments, and not only the mean and variance.

Expression (27) can be mapped onto the common decomposition into ‘intrinsic’ and ‘extrinsic’ components [63, 19], if we note that, in our model, the ‘intrinsic’ components are the downstream processes of transcription and degradation, whose rates are affected by the ‘extrinsic’ variability due to upstream factors. Such upstream factors can be biologically diverse, and can be both intra- and extra-cellular. Therefore throughout this paper we refer to ‘upstream/downstream’ processes instead of ‘intrinsic/extrinsic’ noise, to emphasise that upstream processes can reflect variability that is internal to the cell as well as cell-to-cell variability. For example, the asynchronous stochastic promoter switching described in Sec. 3.2 is an upstream process here, which in the literature might have been classed as ‘intrinsic’ (although in fact, asynchronicity implies an assumption about cell-to-cell variability). On the other hand, the modulated promoter switching in Sec. 3.3 includes both ‘intrinsic’ and ‘extrinsic’ sources of variability, as usually classed in the literature. In our framework, such processes are treated consistently as ‘upstream’ sources of variability.

**Analysis of time-dependent moments:** The relationship (26) between downstream and upstream moments together with the dynamical equation (13) enables us to solve for the time-dependence of the moments of mRNA counts in terms of the moments of the drive:

$$\mathbb{E}[N_t] = \mathbb{E}[X_t] = \int_0^t e^{-\lambda(t-\tau)} \mathbb{E}[M_\tau] d\tau; \quad (28)$$

$$\mathbb{E}[N_t^2] = \mathbb{E}[X_t] + \mathbb{E}[X_t^2] = \mathbb{E}[N_t] + \int_0^t \int_0^t e^{-\lambda(2t-\tau-\sigma)} \mathbb{E}[M_\tau M_\sigma] d\tau d\sigma, \quad (29)$$

where for simplicity we have assumed constant degradation rate  $\lambda$ . (For the most general case with degradation rate  $L_t$ , see for example Ref. [59].) Therefore, the observed moments  $\mathbb{E}[N_t^k]$  from the data can be used to infer the time-dependent moments of the (usually unobserved) upstream drives.

As a motivating example, we consider a recent experiment [8] measuring single-cell time courses of the expression of gene *csaA* in *Dictyostelium discoideum* when driven by a naturally oscillating extracellular cAMP signal. Corrigan and Chubb found that whilst individual single-cell time traces displayed no clear entrainment, with considerable heterogeneity both across time and across the population, there was a clear correlation between the external cAMP phase (measured by proxy through the cell speed) and the population-averaged, time-dependent level of *csaA* transcripts. This suggests that  $\mathbb{E}[N_t]$  could generate precision in cell choices at the population level [8].

The experiment showed that the population-averaged mRNA expression was approximately sinusoidal. Hence, the data can be fitted to the function

$$\mathbb{E}[N_t] = \beta [1 + \alpha \sin(\omega t)]. \quad (30)$$

Assuming constant degradation rate  $\lambda$ , Eqs. (13) and (28) show that the upstream transcription rate is also sinusoidal with the same frequency, yet with a modified amplitude and a phase shift (Fig. 5):

$$\mathbb{E}[M_t] = \beta \left[ \lambda + \alpha \sqrt{\omega^2 + \lambda^2} \sin \left( \omega t + \arctan \left( \frac{\omega}{\lambda} \right) \right) \right]. \quad (31)$$

This is similar to phase relationships in electrical and electronic circuits.

Consistent with Eq. (31), the cAMP phase and  $\mathbb{E}[N_t]$  were measured experimentally to have the same frequency  $\omega \approx 2\pi/5 \approx 1.26 \text{ min}^{-1}$  [8]. The experiments also showed that  $\mathbb{E}[N_t]$  had a mean phase lag of  $9\pi/10$  (equivalent to a delay of  $\approx 2.25 \text{ min}$ ) after the cAMP signal. Using the degradation rate  $\lambda = 0.04 \text{ min}^{-1}$  [35] for gene *csaA*, it follows that the transcriptional phase lag is  $\arctan(\omega/\lambda) = 0.49\pi$ , and signal transduction introduces a phase lag  $\Delta \simeq 9\pi/10 - \pi/2 = 2\pi/5$ , equivalent to a transduction delay  $\Delta/\omega \simeq 1 \text{ min}$ . Hence our results can be used to adjudicate the time scales linked to cAMP signal transduction within the cell.

Our model also clarifies the effect of the degradation rate  $\lambda$  and frequency  $\omega$  in the observed responses. Given the mRNA population average oscillating around a mean value  $\beta$  (30), the (unobserved) transcription rate oscillates with the same frequency  $\omega$  around a value  $\beta\lambda$  and amplitude scaled by  $\sqrt{\omega^2 + \lambda^2}$ . The transcriptional phase lag  $\arctan(\omega/\lambda)$  is bounded between 0 (when  $\omega/\lambda \rightarrow 0$ ) and  $\pi/2$  (when  $\omega/\lambda \rightarrow \infty$ ). Hence, large degradation rates reduce the phase lag and the amplitude of the mRNA oscillations downstream (through the dimensionless factor  $\omega/\lambda$ ), and reduce the mean value of mRNA expression independently of  $\omega$ .

A similar analysis for the correlation function  $\mathbb{E}[M_t M_s]$  can be achieved by solving Eq. (29) numerically for given data.

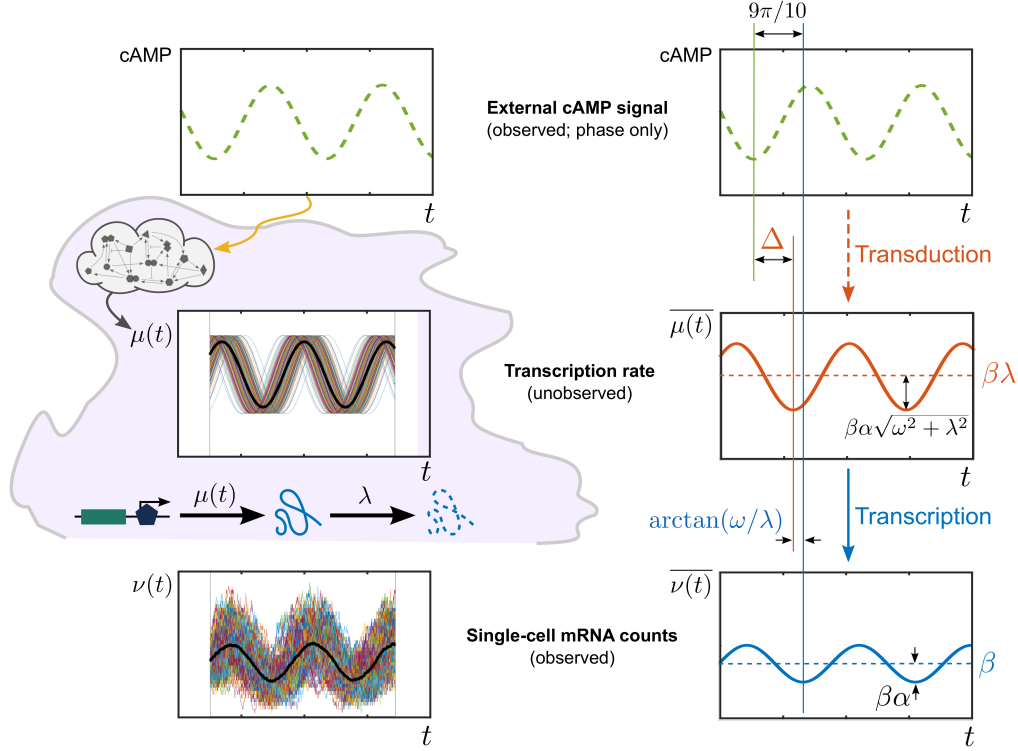


Figure 5: Analysis of single-cell temporal transcription of a gene in response to an upstream oscillatory cAMP signal, motivated by recent experiments [8]. Individual single-cell time courses  $\nu(t)$  of mRNA counts are highly variable with no clear entrainment to the driving signal, whereas the time-dependent ensemble average  $\bar{\nu}(t)$  oscillates with the same frequency as the external drive. This is consistent with Eqs. (30)-(31), which also show that the total phase lag is the resultant of the signal transduction and transcription lags. For a signal with period  $T = 5$  min and a gene with degradation rate  $\lambda = 0.04 \text{ min}^{-1}$  [8], the transcription phase lag is  $\arctan(\omega/\lambda) \simeq \pi/2$ , which corresponds to a delay of  $\simeq 1.25$  min. Given a measured total mean lag of  $9\pi/10$ , this implies that the signal transduction introduces a phase lag  $\Delta \simeq 2\pi/5$ , equivalent to a delay of  $\simeq 1$  min.

## 4.2 Time-dependent ensemble Fano factor: a measure of synchrony in the population

A commonly used measure of variability in the population is the *ensemble Fano factor*:

$$\text{Fano}(N_t) := \frac{\text{Var}(N_t)}{\mathbb{E}[N_t]}, \quad (32)$$

which is unity for the Poisson distribution. Its use has been popularised as a measure of the deviation from the stationary solution of the transcription of an unregulated gene with constant rates [65, 47], which is Poisson; hence with  $\text{Fano}(N_t) \equiv 1, \forall t$ .

For time-varying systems, however, the ensemble Fano factor conveys how the dynamic variability in single cells combines at the population level. Indeed,  $\text{Fano}(N_t)$  can be thought of as a measure of

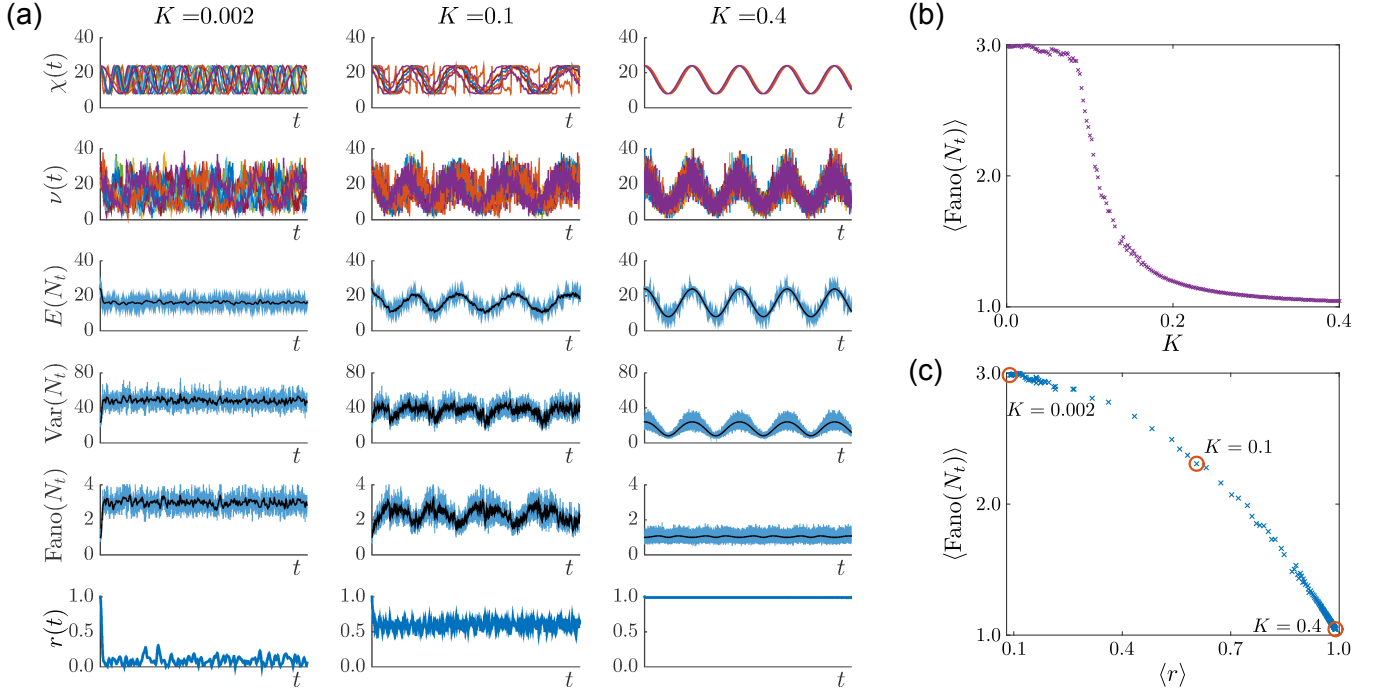


Figure 6: Noise characteristics of the Kuramoto promoter model (18). (a) Numerical simulations for  $C = 100$  oscillatory cells and different coupling parameters:  $K = 0.002, 0.1, 0.4$  (left, middle, right columns). For each coupling, the sample paths of the upstream effective drive  $X$  and mRNA counts  $N$  are shown. The mean, variance, and ensemble Fano factor of  $N$  were calculated from the sample paths of  $N$  (blue lines) and, more efficiently, from the sample paths of  $X$  (black lines). The last row shows the Kuramoto order parameter  $r(t)$  measuring the cell synchrony, signaled by  $r(t) \rightarrow 1$ . (b) Ensemble Fano factor (averaged over the simulated time courses) against coupling parameter  $K \in (0, 0.4]$ . As  $K$  is increased, the oscillators become synchronised and the ensemble Fano factor decreases towards the Poisson value of unity. (c) Scatter plot of the ensemble Fano factor against the order parameter  $r(t)$  (both averaged over the simulated time courses). As the oscillators become synchronised ( $\langle r \rangle \rightarrow 1$ ), the ensemble Fano factor also approaches 1, signifying that the distribution is Poissonian at all times.

synchrony in the population at time  $t$ . For instance, it follows from Eq. (10) that the ensemble Fano factor for a population with perfectly synchronous drives is always equal to one,  $\text{Fano}(N_t) \equiv 1, \forall t$ . Even if the upstream drive  $\chi(t)$  changes in time, the population remains synchronous and has a Poisson distribution at all times. On the other hand, under the assumptions of our model, when  $\text{Fano}(N_t)$  varies in time it reflects a change in the degree of synchrony between cells, as captured by the upstream drive  $X_t$ . Indeed, from (26) it follows that:

$$\text{Fano}(N_t) := \frac{\text{Var}(N_t)}{\mathbb{E}[N_t]} = \frac{\text{Var}(X_t) + \mathbb{E}[X_t]}{\mathbb{E}[X_t]} = 1 + \text{Fano}(X_t).$$

The greater the synchrony at time  $t$ , the closer  $\text{Fano}(N_t)$  is to unity, since the deviation from the Poisson

distribution emanates from the ensemble Fano factor of the upstream drive  $X_t$ .

As an example, consider the Kuramoto promoter model (18)-(19) introduced in Section 3.1.2, where the cells in the population become more synchronised as the value of the coupling  $K$  is increased. Figure 6 shows simulation results for 100 cells with a range of couplings. The order parameter  $r(t) \in [0, 1]$  measures the phase coherence of the oscillators at time  $t$ ; as it grows closer to 1, so grows the degree of synchrony. Using the Kuramoto numerics, we calculate the ensemble Fano factor  $\text{Fano}(N_t)$  for the transcription model. As seen in Fig. 6(b)-(c), the more synchronous, the closer the Fano factor is to the Poisson value, i.e.,  $\langle r(t) \rangle \rightarrow 1 \implies \langle \text{Fano}(N_t) \rangle \rightarrow 1$ .

Figure 6 also illustrates the computational advantages of our method. The cost to approximate the time-varying ensemble moments is drastically reduced by using (26), because transcription and degradation events do not have to be simulated. The sample paths of the effective drive  $\chi_i(t)$  were used to estimate the time-varying moments:  $\mathbb{E}[N_t] = \mathbb{E}[X_t]$  and  $\text{Var}(N_t) = \text{Var}(X_t) + \mathbb{E}[X_t]$  (shown in black). These correspond to the numerical simulation of ODEs, and are far more efficient than sampling from realisations  $\nu_i(t)$  of the mRNA copy number.

## 5 Variability over time: stationarity and ergodicity

Our results up to now have *not* assumed stationarity; in general, the distribution (14) and moments (26) depend on time. If the cells in the population are uncorrelated and both  $M$  and  $L$  are *stationary* (i.e., their statistics do not change over time) then  $f_{X_t}(x, t)$  tends to a stationary density  $f_{X_t}(x)$  [59], and the full solution  $P(n, t)$  also tends to a stationary distribution  $P(n)$ .

Under such assumptions leading to stationarity, any time dependence in  $P(n, t)$  only describes the ‘burn-in’ transient from an initial condition towards the attracting stationary distribution, as discussed above in Section 2.1. Several examples of such transience have been studied in the literature, both in gene-state switching models with constant rate parameters [21, 54, 69], and in a model with state-dependent rates [58], to describe how the distribution  $P(n, t)$  settles to stationarity when the process is started from an initial Kronecker delta distribution  $P(n, 0) = \delta_{n0}$ . Figure 7 and Appendix A.2 analyse this transience explicitly for the random telegraph model.

If, in addition to stationarity, we assume the cells to be indistinguishable, the population is *ergodic*. In this case, the distribution obtained from a single cell over a time  $T$ , as  $T \rightarrow \infty$ , is equivalent to the distribution obtained from a time snapshot at stationarity of a population of  $C$  cells, as  $C \rightarrow \infty$ , i.e.,

$$P(n) = \langle P(n) \rangle \quad (33)$$

$$\text{where } P(n) := \lim_{t \rightarrow \infty} P(n, t) = \lim_{t \rightarrow \infty} \lim_{C \rightarrow \infty} \frac{1}{C} \sum_{i=1}^C \frac{\chi_i(t)^n}{n!} e^{-\chi_i(t)} f_{X_t}(\chi_i(t), t) = \int \frac{x^n}{n!} e^{-x} f_{X_t}(x) dx, \quad (34)$$

$$\text{and } \langle P(n) \rangle := \lim_{T \rightarrow \infty} \frac{1}{T} \int_0^T P(n, t | \chi(t)) dt = \lim_{T \rightarrow \infty} \frac{1}{T} \int_0^T \frac{\chi(t)^n}{n!} e^{-\chi(t)} dt. \quad (35)$$

Here,  $\langle \cdot \rangle$  denotes time-averaging, and  $\chi(t)$  in Eq. (35) is the sample path of the effective drive for a randomly chosen cell. Therefore, under the assumption of ergodicity, the averages computed over single-cell sample paths can be used to estimate the stationary distribution of the population.

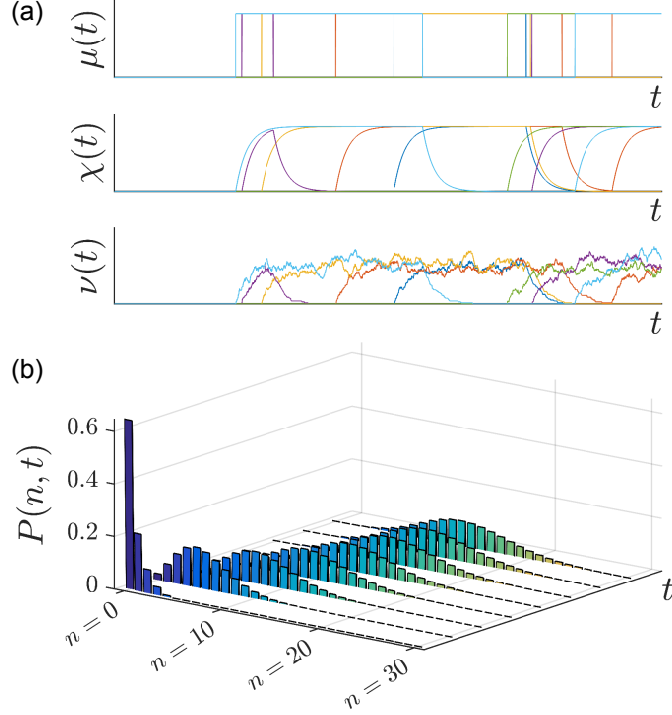


Figure 7: ‘Burn-in’ transient in the random telegraph (RT) model. (a) Sample paths of the transcription rate  $M$ , the effective upstream drive  $X$ , and the number of mRNAs  $N$  for an initial condition  $P(0, 0) = 1$  with all cells initialised in the inactive state [21]. (b) The full solution of the RT model for this initial probability distribution exhibits an exponential decay as the system approaches its stationary distribution. The delta distribution at  $t = 0$  is omitted for scaling purposes.

### 5.1 Ergodic systems: stochastic *vs* deterministic drives

It has been suggested that stochastic and periodic drives lead to distinct properties in the noise characteristics within a cell population [19]. We investigate the effect of different temporal drives on the full distribution (14) under ergodicity using (33)-(35). Note that when  $\chi(t)$  is periodic with period  $T$ , the limit in Eq. (35) is not required. In Figure 8, we show the time-averaged distribution  $\langle P(n) \rangle$  for a cell under three different upstream drives  $\mu(t)$ : (i) a continuous sinusoidal form; (ii) a discontinuous square wave form; (iii) a random telegraph (RT) form, which can be thought of as the stochastic analogue of the square wave. In all cases, the drive  $\{\mu(t)\}_{t \geq 0} \in [0, 20]$  with the same period, or expected period,  $T$ . For simplicity, we set  $\lambda(t) \equiv 1$ .

As the period  $T$  is varied, the similarity between the distributions under the three upstream drives varies considerably (Fig. 8). At small  $T$ , the distributions under sinusoidal and square wave forms are most similar; whereas at large  $T$ , the distributions under square wave and RT forms become most similar. In general, the distribution of the RT model has longer tails (i.e.,  $n$  low and high) as a consequence of long (random) waiting times that allow the system to reach equilibrium in the active and inactive states,

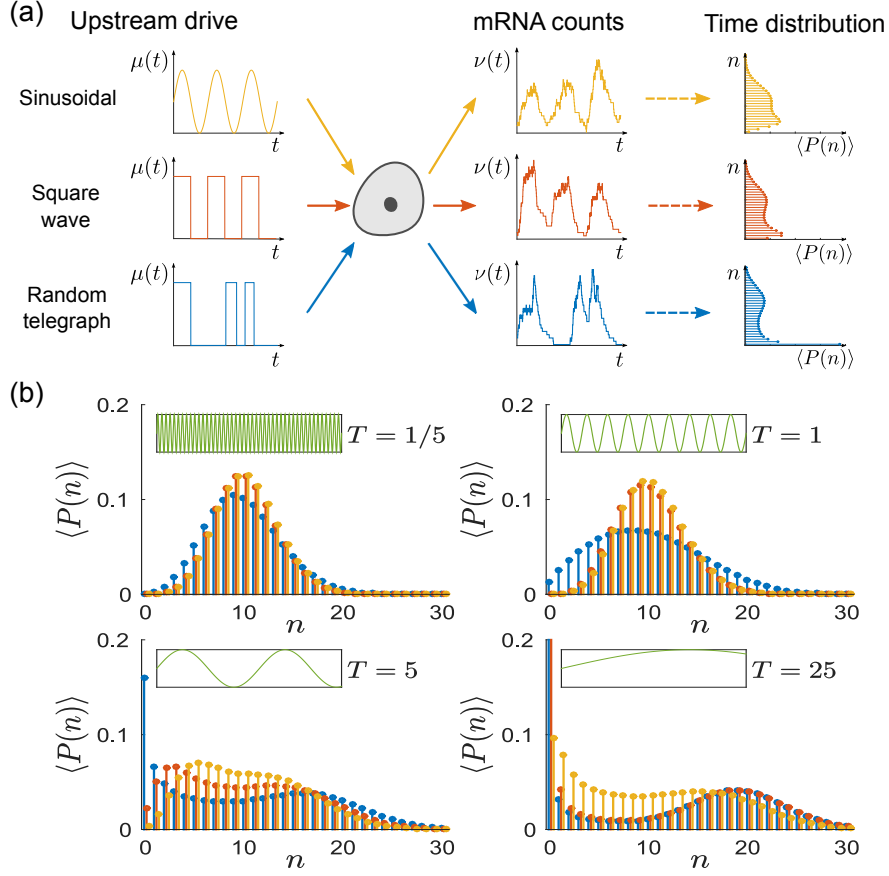


Figure 8: Ergodic transcription models under periodic and stochastic upstream drives. (a) We consider gene transcription under three drives  $\mu(t) \in [0, 20]$ : a sinusoidal wave with period  $T$  (yellow); a square wave with period  $T$  (red); a random telegraph process with expected waiting time  $T/2$  in each state (blue). For such ergodic systems, the distribution computed over time  $\langle P(n) \rangle$  corresponds to the stationary distribution. (b) The distribution  $\langle P(n) \rangle = P(n)$  presents distinct features as the period  $T$  is varied.

although this effect is less pronounced when the promoter switching is fast relative to the time scales of transcription and degradation (e.g.,  $T = 1/5$ ). On the other hand, as  $T$  grows, the square wave and RT drives are slow and the system is able to reach the equilibrium in both active and inactive states. Hence the probability distributions of the square wave and RT drives become similar, with a more prominent bimodality.

## 5.2 The temporal Fano factor: windows of stationarity in single-cell time course data

The *temporal Fano factor* (TFF) is defined similarly to the ensemble version (32), but is calculated from the variance and mean of a *single time series*  $\{\nu(t)\}_{t \geq 0}$  over a time window  $W := (t_1, t_2)$ :

$$\text{TFF}_{\{\nu(t)\}}(W) := \frac{\langle \nu(t)^2 \rangle_{t \in W} - \langle \nu(t) \rangle_{t \in W}^2}{\langle \nu(t) \rangle_{t \in W}}. \quad (36)$$

In fact, this is the original definition of the Fano factor [13], which is used in signal processing to estimate statistical fluctuations of a count variable over a time window. Although  $N_t$  is not a count variable (it decreases with degradation events), the TFF can be used to detect windows of stationarity in single-cell time courses.

Figure 9a shows a single-cell sample path  $\{\nu(t)\}_{t \geq 0}$  generated by the (leaky) random telegraph model with constant degradation rate  $\lambda$ , and transcription rates  $\mu_1 > \mu_0 > 0$  for the active and inactive promoter states. The leaky RT model is equivalent to the standard RT model, and switches between two states with expectations  $\mu_1/\lambda$  and  $\mu_0/\lambda$ . In the time windows  $W$  between promoter switching,  $\{\nu(t)\}_{t \in W}$  can be considered almost at stationarity and described by a Poisson distribution with parameter  $\mu_0/\lambda$  (resp.  $\mu_1/\lambda$ ) in the inactive (resp. active) state. Hence  $\text{TFF}_{\{\nu(t)\}}(W) \simeq 1$  across most of the sample path, except over the short transients  $W_{\text{trans}}$  when the system is switching between states, where  $\text{TFF}_{\{\nu(t)\}}(W_{\text{trans}}) > 1$  (Fig. 9b).

Alternatively, this information can be extracted robustly from the *cumulative Fano factor* (cTFF):

$$\text{cTFF}_{\{\nu(t)\}}(t_1, t) = \text{TFF}_{\{\nu(t)\}}((t_1, t)), \quad t \geq t_1 \quad (37)$$

which is computed over a *growing window* from a fixed starting time  $t_1$ . The cTFF is a cumulative moving average giving an integrated description of how the stationary regimes are attained between switching events indicated by the step-like structure of the heatmap in Fig. 9c.

## 6 Discussion

We have presented the solution of the master equation for gene transcription with upstream dynamical variability in a setting that allows a unified treatment of a broad class of models, enabling quantitative biologists to go beyond stationary solutions when analysing noise sources in single-cell experiments. As a complementary approach to the explicit stochastic simulation of networks with many genes to account for the variability in data, our work uses a parsimonious transcription model of Poissonian type that includes explicitly the effect of dynamical and cell-to-cell upstream variability in the master equation. We show that the solution to this gene transcription-degradation model can be expressed as a Poisson mixture form (14). This solution can be interpreted as the combination of an upstream component (dynamic or static; deterministic or stochastic) with a downstream Poissonian immigration-death process. Since only the upstream process is model-specific, different models are solved by obtaining the different mixing densities  $f_{X_t}$  of the upstream process. This generic mathematical structure can describe both time-dependent snapshots across the population, as well as the dynamical variability over single-cell time courses in a coherent fashion.

The solution (14) can also be understood from the perspective of Gardiner and Chaturvedi's *Poisson representation* [17, 16]. Originally, the Poisson representation was introduced as an *ansatz* for asymptotic

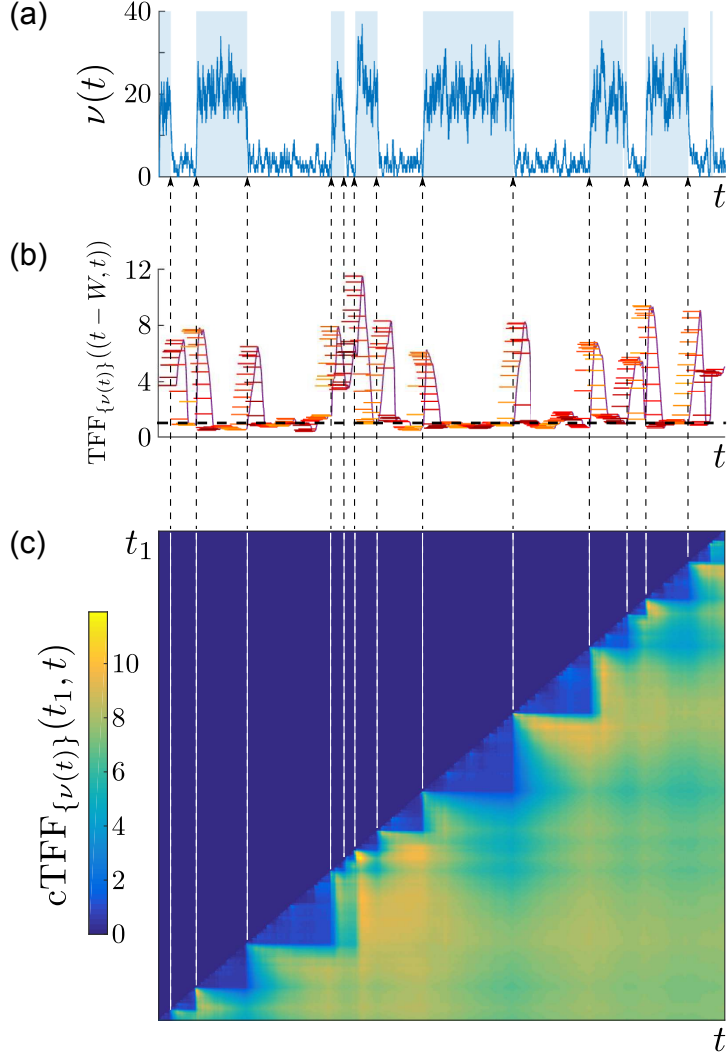


Figure 9: The temporal and cumulative Fano factor. (a) A sample path  $\{\nu(t)\}_{t \geq 0}$  of mRNA counts from the (leaky) RT model. The time periods when the gene is in the active state are shaded. (b) The temporal Fano factor (36),  $\text{TFF}_{\{\nu(t)\}}((t-W, t))$ , computed over a time window  $W$  of fixed length indicated by the horizontal bars at each  $t$ . When  $W$  extends over a stationary section of the sample path, TFF is close to unity, corresponding to the Poisson distribution (black dashed line). (c) Heatmap of the cumulative Fano factor (37),  $\text{cTFF}_{\{\nu(t)\}}(t_1, t)$ , defined only for  $t \geq t_1$ . Note the marked step pattern corresponding to the switching times, indicated by dashed lines as a guide to the eye.

expansions of stationary systems, and included only constant rate parameters. Hence the original Poisson representation *ansatz* has not been used widely for time-varying solutions [17]. In contrast, our time-dependent Poisson mixture (14) is obtained here as a solution to a non-stationary ME model, rather than

backwards via basis expansions, and the mixing density  $f_{X_t}$  has a physical interpretation in terms of single-cell sample paths relatable to data.

In this respect, our preparatory result (8) for the perfectly synchronous population can be thought of as an extension of the ‘Poisson representation’ to include time-varying rate parameters. Note also that this perfectly synchronous solution (8) corresponds to a particular case of the multi-gene solution obtained by Jahnke and Huisinga [24]. However, (8) does not yet encapsulate the cell-to-cell variability. It is the full Poisson mixture solution (14) that extends the scope of the time-varying ‘Poisson representation’ a step further, by allowing for stochastic rate parameters that can describe cell-to-cell variability as well as dynamic variability.

Our solution confers two broad advantages. The first is pragmatic: Since  $X_t$  is a continuous random variable satisfying a linear random differential equation, we can draw upon the rich theory and analytical results for  $f_{X_t}$ , even for non-stationary models, or we can use ODE and PDE solvers as further options to solve the differential equation for  $f_{X_t}$ . If simulations are still necessary, sampling  $P(n, t|M, L)$  directly using stochastic simulation algorithms becomes computationally expensive, particularly if the upstream processes  $M$  and  $L$  are time-varying [53]. Instead, we can sample  $f_{X_t}(x, t)$  directly using the random differential equation (13), and then obtain the full distribution via numerical integration using (14). This approach leads to a significant reduction in computational cost, as shown in Fig. 10.

Our approach can also be used to analyse noise characteristics in conjunction with biological hypotheses. If measurements of additional cellular variables (e.g., cell cycle) are available, they can be incorporated as a source of variability for gene regulation to test biological hypotheses computationally against experimental data. Conversely, it is possible to discount the Poissonian component from observed data, so as to fit different promoter models to experimental data and perform model comparison [10]. Our discussion of a recent experiment of gene expression driven by cAMP signalling [8] exemplifies this approach.

The second advantage of our framework is conceptual. Through the natural decoupling of the solution into a discrete, Poisson component (‘downstream’) and a continuous, mixing component (‘upstream’), we derive time-dependent expressions for both ensemble and temporal moments, recasting the concept of ‘intrinsic’/‘extrinsic’ noise for dynamic upstream cellular drives. Importantly, all upstream variability gets effectively imbricated through the upstream effective drive  $X$ , which can be interpreted in terms of a biochemical differential rate equation. This analysis clarifies how upstream fluctuations are combined to affect the probability distribution of the mRNA copy number, providing further intuition about the sources of noise and their temporal characteristics. Indeed, stripping the model down to its extrinsic component  $f_{X_t}$  can provide us with additional understanding of its structure and time scales [10].

Finally, although we have concentrated here on the amenable analytical solutions that can be obtained for the single gene case, we remark that our solution could be extended to monomolecular multi-gene networks, by merging Jahnke and Huisinga’s result [24] for synchronous networks with our mixture result for the asynchronous case. Such a generalisation could be implemented computationally to reduce the cost of simulating stochastic networks. Such an extension will be the subject of future work. The solutions of higher order reaction systems obtained through the Poisson representation *ansatz* could also be extended to include stochastic rates. This approach could lead to deeper understanding of models with and without feedback [22].

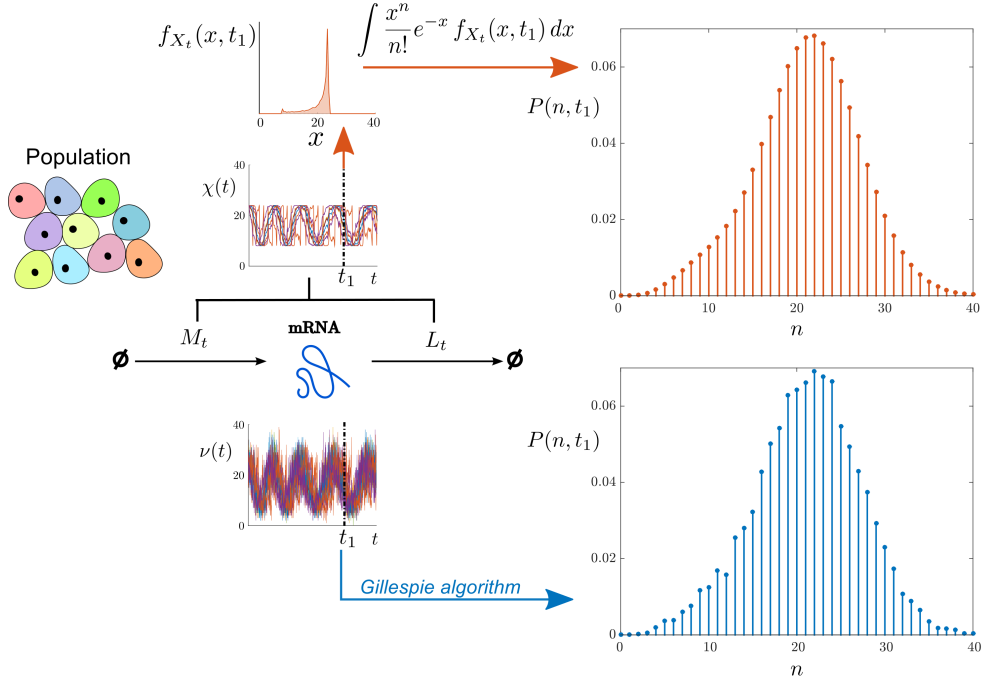


Figure 10: Efficient sampling of the full distribution  $P(n, t)$  for transcription with upstream cellular drives. We consider upstream drives governed by the Kuramoto promoter model (18) for  $C = 10,000$  coupled oscillatory cells. Sample paths of  $N$  are simulated directly with the Gillespie algorithm to approximate  $P(n, t)$  at time  $t_1$  (bottom, blue). Alternatively, sample paths of  $X$  are used to estimate  $f_{X_t}$ , which is then mixed by performing the numerical integration (14) to obtain  $P(n, t)$  (top, red). The latter sampling through  $X$  is more regular and far less costly: CPU time via  $N$  is  $\approx 36000$  s whereas CPU time via  $X$  is  $\approx 0.1$  s.

## Acknowledgments

We are grateful for insightful comments and extended discussions with Juan Kuntz, Philipp Thomas, Martin Hemberg and Andrew Parry. JD was funded by an EPSRC PhD studentship. MB acknowledges funding from the EPSRC through grants EP/I017267/1 and EP/N014529/1.

**Authors' contributions:** JD carried out the calculations and simulations, participated in the design of the study, and wrote the manuscript. MB conceived of the study, designed the study, coordinated the study, and wrote the manuscript. Both authors gave final approval for publication.

**Data statement:** No new data was collected in the course of this research.

## References

- [1] M. Abramowitz and I. A. Stegun. *Handbook of mathematical functions*. Dover, 1964.
- [2] J. Almquist, L. Bendrioua, C. B. Aliels, M. Goksör, S. Hohmann, and M. Jirstrand. A nonlinear mixed effects approach for modeling the cell-to-cell variability of Mig1 dynamics in yeast. *PLoS ONE*, 10(4):e0124050, 2015.
- [3] G. Balázsi, A. van Oudenaarden, and J. J. Collins. Cellular decision making and biological noise: From microbes to mammals. *Cell*, 144(6):910–925, 2011.
- [4] J. Bieler, R. Cannavo, K. Gustafson, C. Gobet, D. Gatfield, and F. Naef. Robust synchronization of coupled circadian and cell cycle oscillators in single mammalian cells. *Molecular Systems Biology*, 10(7), 2014.
- [5] C. G. Bowsher and P. S. Swain. Identifying sources of variation and the flow of information in biochemical networks. *Proceedings of the National Academy of Sciences*, 109(20):E1320–E1328, 2012.
- [6] P. Brémaud. *Markov chains, Gibbs fields, Monte Carlo simulation and queues*. Springer, 2001.
- [7] H. H. Chang, M. Hemberg, M. Barahona, D. E. Ingber, and S. Huang. Transcriptome-wide noise controls lineage choice in mammalian progenitor cells. *Nature*, 453:544–547, 2008.
- [8] A. M. Corrigan and J. R. Chubb. Regulation of transcriptional bursting by a naturally oscillating signal. *Current Biology*, 24(205-211), 2014.
- [9] N. Crosetto, M. Bienko, and A. van Oudenaarden. Spatially resolved transcriptomics and beyond. *Nature Reviews Genetics*, 16:57–66, 2015.
- [10] J. Dattani. PhD thesis, Imperial College London, 2016.
- [11] S. G. Eick, W. A. Massey, and W. Whitt. Physics of the  $M_t/G/\infty$  queue. *Operations Research*, 41(4):731–742, 1993.
- [12] M. B. Elowitz, A. J. Levine, E. D. Siggia, and P. S. Swain. Stochastic gene expression in a single cell. *Science*, 297:1183–1186, 2002.
- [13] U. Fano. Ionization yield of radiations. II. the fluctuations of the number of ions. *Physical Review*, 72(1):26–29, 1947.
- [14] J. Garcia-Ojalvo and A. M. Arias. Towards a statistical mechanics of cell fate decisions. *Current opinion in genetics & development*, 22(6):619–626, 2012.
- [15] J. Garcia-Ojalvo, M. B. Elowitz, and S. H. Strogatz. Modeling a synthetic multicellular clock: Repressilators coupled by quorum sensing. *Proceedings of the National Academy of Sciences*, 101(30):10955–10960, 2004.
- [16] C. W. Gardiner. *Handbook of stochastic methods*. Springer, 2nd edition, 1985.

- [17] C. W. Gardiner and S. Chaturvedi. The Poisson representation. I. A new technique for chemical master equations. *Journal of Statistical Physics*, 17(6):429–468, 1977.
- [18] J. Hasenauer, V. Wolf, A. Kazeroonian, and F. J. Theis. Method of conditional moments (MCM) for the chemical master equation. *Journal of Mathematical Biology*, 69:687–735, 2014.
- [19] A. Hilfinger and J. Paulsson. Separating intrinsic from extrinsic fluctuations in dynamic biological systems. *Proceedings of the National Academy of Sciences*, 108(29):12167–12172, 2011.
- [20] J. E. M. Hornos, D. Schultz, G. C. P. Innocentini, J. Wang, A. M. Walczak, J. N. Onuchic, and P. G. Wolynes. Self-regulating gene: an exact solution. *Physical Review E*, 72:051907, 2005.
- [21] S. Iyer-Biswas, F. Hayot, and C. Jayaprakash. Stochasticity of gene products from transcriptional pulsing. *Physical Review E*, 79:031911, 2009.
- [22] S. Iyer-Biswas and C. Jayaprakash. Mixed Poisson distributions in exact solutions of stochastic autoregulation models. *Physical Review E*, 90:052712, 2014.
- [23] A. Jadbabaie, N. Motee, and M. Barahona. On the stability of the kuramoto model of coupled nonlinear oscillators. In *IEEE American Control Conference, 2004*, volume 5, pages 4296–4301. IEEE, 2004.
- [24] T. Jahnke and W. Huisinga. Solving the chemical master equation for monomolecular reaction systems analytically. *Journal of Mathematical Biology*, 54(1):1–26, 2007.
- [25] J. P. Junker and A. van Oudenaarden. Every cell is special: Genome-wide studies add a new dimension to single-cell biology. *Cell*, 157(1):8–11, Mar. 2014.
- [26] M. Ko. A stochastic model for gene induction. *Journal of Theoretical Biology*, 153:181–194, 1991.
- [27] S. Konermann, M. D. Brigham, A. Trevino, P. D. Hsu, M. Heidenreich, L. Cong, R. J. Platt, D. A. Scott, G. M. Church, and F. Zhang. Optical control of mammalian endogenous transcription and epigenetic states. *Nature*, 500:472–476, 2013.
- [28] N. Kumar, T. Platini, and R. V. Kulkarni. Exact distributions for stochastic gene expression models with bursting and feedback. *Physical Review Letters*, 113:268105, 2014.
- [29] Y. Kuramoto. Self-entrainment of a population of coupled non-linear oscillators. In *International Symposium on Mathematical Problems in Theoretical Physics*, volume 39 of *Lecture notes in Physics*, pages 420–422. Springer Berlin Heidelberg, 1975.
- [30] M. Levine and R. Tjian. Transcription regulation and animal diversity. *Nature*, 424:147–151, 2003.
- [31] S. Lück, K. Thurley, P. F. Thaben, and P. O. Westermark. Rhythmic degradation explains and unifies circadian transcriptome and proteome data. *Cell Reports*, 9:741–751, 2014.
- [32] H. Maamar, A. Raj, and D. Dubnau. Noise in gene expression determines cell fate in *Bacillus subtilis*. *Science*, 317:526–529, 2007.

- [33] I. Mihalcescu, W. Hsing, and S. Leibler. Resilient circadian oscillator revealed in individual cyanobacteria. *Nature*, 430(6995):81–5, 2004.
- [34] N. Molina, D. M. Suter, R. Cannava, B. Zoller, I. Gotic, and F. Naef. Stimulus-induced modulation of transcriptional bursting in a single mammalian gene. *Proceedings of the National Academy of Sciences*, 110(51):20563–20568, 2013.
- [35] T. Muramoto, D. Cannona, M. Gierliński, A. Corrigan, G. J. Barton, and J. R. Chubb. Live imaging of nascent RNA dynamics reveals distinct types of transcriptional pulse regulation. *Proceedings of the National Academy of Sciences*, 109(19):7350–7355, 2012.
- [36] P. J. Murray, P. K. Maini, and R. E. Baker. The clock and wavefront model revisited. *Journal of Theoretical Biology*, 283(1):227–238, 2011.
- [37] N. D. L. Owens, I. L. Blitz, M. A. Lane, I. Patrushev, J. D. Overton, M. J. Gilchrist, K. W. Y. Cho, and M. K. Khoka. Measuring absolute RNA copy numbers at high temporal resolution reveals transcriptome kinetics in development. *Cell Reports*, 14(3):632–647, 2016.
- [38] H. Y. Park, H. Lim, Y. J. Yoon, A. Follenzi, C. Nwokafor, M. Lopez-Jones, X. Meng, and R. H. Singer. Visualization of dynamics of single endogenous mRNA labeled in live mouse. *Science*, 343(6169):422–424, 2014.
- [39] P. Paszek. Modeling stochasticity in gene regulation: Characterization in the terms of the underlying distribution function. *Bulletin of Mathematical Biology*, 69:1567–1601, 2007.
- [40] J. Paulsson. Models of stochastic gene expression. *Physics of life reviews*, 2:157–175, 2005.
- [41] R. Pawula. Generalizations and extensions of the Fokker-Planck-Kolmogorov equations. *IEEE Transactions on Information Theory*, 13(1):33–41, January 1967.
- [42] R. Pawula. The transition probability density function of the low-pass filtered random telegraph signal. *International Journal of Control*, 12(1):25–32, March 1970.
- [43] J. Peccoud and B. Ycart. Markovian modeling of gene-product synthesis. *Theoretical Population Biology*, 48(2):222–234, 1995.
- [44] H. Pendar, T. Platini, and R. V. Kulkarni. Exact protein distributions for stochastic models of gene expression using partitioning of poisson processes. *Physical Review E*, 87:042720, 2013.
- [45] A. Raj, C. S. Peskin, D. Tranchina, D. Y. Vargas, and S. Tyagi. Stochastic mRNA synthesis in mammalian cells. *PLoS Biology*, 4(10):1707–1719, 2006.
- [46] A. Raj and A. van Oudenaarden. Nature, nurture, or chance: stochastic gene expression and its consequences. *Cell*, 135(2):216–226, 2008.
- [47] A. Raj and A. van Oudenaarden. Single-molecule approaches to stochastic gene expression. *Annual review of biophysics*, 38:255–70, Jan. 2009.

- [48] J. Riordan. Moment recurrence relations for binomial, poisson and hypergeometric frequency distributions. *The Annals of Mathematical Statistics*, 8(2):103–111, 1937.
- [49] A. Sánchez, H. G. Garcia, D. Jones, R. Phillips, and J. Kondev. Effect of promoter architecture on the cell-to-cell variability in gene expression. *PLoS Computational Biology*, 105(13):5081–5086, 2008.
- [50] A. Sánchez and I. Golding. Genetic determinants and cellular constraints in noisy gene expression. *Science*, 342:1188–1193, 2013.
- [51] A. Sánchez and J. Kondev. Transcriptional control of noise in gene expression. *Proceedings of the National Academy of Sciences*, 105(13):5081–5086, 2008.
- [52] A. Senecal, B. Munsky, F. Proux, N. Ly, F. E. Braye, C. Zimmer, F. Mueller, and X. Darzacq. Transcription factors modulate c-Fos transcriptional bursts. *Cell Reports*, 8:75–83, 2014.
- [53] V. Shahrezaei, J. F. Olivier, and P. S. Swain. Colored extrinsic fluctuations and stochastic gene expression. *Molecular Systems Biology*, 4(196), 2008.
- [54] V. Shahrezaei and P. S. Swain. Analytical distributions for stochastic gene expression. *Proceedings of the National Academy of Sciences*, 105(45):17256–17261, 2008.
- [55] Z. S. Singer, J. Yong, J. Tischler, J. A. Hackett, A. Altinok, M. A. Surani, L. Cai, and M. B. Elowitz. Dynamic heterogeneity and DNA methylation in embryonic stem cells. *Molecular Cell*, 55(2):319 – 331, 2014.
- [56] L. J. Slater. *Generalized Hypergeometric Functions*. Cambridge University Press, 1966.
- [57] M. W. Smiley and S. R. Proulx. Gene expression dynamics in randomly varying environments. *Journal of Mathematical Biology*, 61:231–251, 2010.
- [58] S. Smith and V. Shahrezaei. General transient solution of the one-step master equation in one dimension. *Physical Review E*, 91:062119, 2015.
- [59] T. T. Soong. *Random Differential Equations in Science and Engineering*, volume 103 of *Mathematics in Science and Engineering*. Academic Press, 1973.
- [60] S. H. Strogatz. From Kuramoto to Crawford: exploring the onset of synchronization in populations of coupled oscillators. *Physica D: Nonlinear Phenomena*, 143:1–20, 2000.
- [61] Y. F. Suprunenko, P. T. Clemson, and A. Stefanovska. Chronotaxic systems: A new class of self-sustained nonautonomous oscillators. *Physical Review Letters*, 111:024101, 2013.
- [62] D. M. Suter, N. Molina, D. Gatfield, K. Schneider, U. Schibler, and F. Naef. Mammalian genes are transcribed with widely different bursting kinetics. *Science*, 332:472–474, 2011.
- [63] P. S. Swain and M. B. Elowitz. Intrinsic and extrinsic contributions to stochasticity in gene expression. *Proceedings of the National Academy of Sciences*, 99(20):12795–12800, 2002.

- [64] A. F. Taylor, M. R. Tinsley, F. Wang, Z. Huang, and K. Showalter. Dynamical quorum sensing and synchronization in large populations of chemical oscillators. *Science*, 323(5914):614–617, 2009.
- [65] M. Thattai and A. van Oudenaarden. Intrinsic noise in gene regulatory networks. *Proceedings of the National Academy of Sciences*, 98(15):8614–8619, 2001.
- [66] P. Todorovic. *An Introduction to Stochastic Processes and their Applications*. Springer, 1992.
- [67] K. Uriu, S. Ares, A. C. Oates, and L. G. Morelli. Optimal cellular mobility for synchronization arising from the gradual recovery of intercellular interactions. *Physical Biology*, 9(3):036006, 2012.
- [68] N. G. van Kampen. *Stochastic processes in physics and chemistry*. Elsevier, 2nd edition, 1992.
- [69] Y. Vandecan and R. Blossey. Self-regulatory gene: An exact solution for the gene gate model. *Physical Review E*, 87:042705, 2013.
- [70] P. Visco, R. J. Allen, and M. R. Evans. Exact solution of a model DNA-inversion genetic switch with orientational control. *Physical Review Letters*, 101:118104, 2008.
- [71] D. J. Wilkinson. Stochastic modelling for quantitative description of heterogeneous biological systems. *Nature Reviews Genetics*, 10:122–133, 2009.
- [72] L. Wolf, O. K. Silander, and E. van Nimwegen. Expression noise facilitates the evolution of gene regulation. 4:e05856, 2015.
- [73] J. W. Young, J. C. W. Locke, A. Altinok, N. Rosenfeld, T. Bacarian, P. S. Swain, E. Mjolsness, and M. B. Elowitz. Measuring single-cell gene expression dynamics in bacteria using fluorescence time-lapse microscopy. *Nature Methods*, 7(1):80–88, 2012.
- [74] C. Zechner and H. Koepl. Uncoupled analysis of stochastic reaction networks in fluctuating environments. *PLOS Computational Biology*, 10(12):e1003942, 2014.
- [75] E. S. Zeron and M. Santillán. *Numerical solution of the Chemical Master Equation: Uniqueness and stability of the stationary distribution for chemical networks, and mRNA bursting in a gene network with negative feedback regulation*, volume 487, chapter 6. Elsevier, 2011.
- [76] J. Zhang, L. Chen, and T. Zhou. Analytical distribution and tunability of noise in a model of promoter progress. *Biophysical Journal*, 102:1247–1257, 2012.
- [77] B. Zoller, D. Nicolas, N. Molina, and F. Naef. Structure of silent transcription intervals and noise characteristics of mammalian genes. *Molecular Systems Biology*, 11(823), 2015.

## Appendices

### A The ‘burn-in’ transient towards stationarity

In Section 2.1, it was stated that the contribution from the initial condition  $N_t^{ic}$  decreases exponentially for biophysically realistic degradation rates  $\{\lambda(t)\}_{t \geq 0}$ . As a result, the transcripts that were present at  $t = 0$  are expected to degrade in finite time, and the long-term population is expected to be composed only of mRNA molecules that were transcribed since  $t = 0$ .

Let the initial condition be described by a random variable  $N_0$  with a given probability distribution. It follows from Eqs (8)-(9) that

$$\begin{aligned}
 P(n, t | \{\mu(\tau)\}_{\tau \in [0, t]}, \{\lambda(\tau)\}_{\tau \in [0, t]}) &= \sum_{n_0} P(n, t | \{\mu(\tau)\}_{\tau \in [0, t]}, \{\lambda(\tau)\}_{\tau \in [0, t]}, n_0) \Pr(N_0 = n_0) \\
 &= \sum_{n_0} \sum_{k=0}^n \Pr(N_t^{ic} = k | N_0 = n_0) \Pr(N_t^s = n - k) \Pr(N_0 = n_0) \\
 &= \sum_{k=0}^n \Pr(N_t^s = n - k) \left[ \sum_{n_0} \Pr(N_t^{ic} = k | N_0 = n_0) \Pr(N_0 = n_0) \right] \\
 &= \sum_{k=0}^n \Pr(N_t^s = n - k) \Pr(N_t^{ic} = k),
 \end{aligned}$$

where  $N_t^{ic}|n_0$  and  $N_t^s$  are distributed according to Eqs (5)-(7), and  $\Pr(N_t^{ic} = k)$  is the mixture of the time-dependent binomial distribution (5) and the distribution of the initial condition  $N_0$ .

#### A.1 ‘Burn-in’ transience in the model with constant transcription and degradation

##### The decay towards stationarity

To understand the ‘burn-in’ period more explicitly, consider the simplest example of the gene transcription model (1) with constant transcription and degradation rates  $\mu$  and  $\lambda$ , and assume that there are initially  $n_0$  mRNA transcripts. Given that  $N_0 \sim \delta_{0, n_0}$ , the solution is given by:

$$\begin{aligned}
 N_t &= N_t^{ic}|n_0 + N_t^s \quad \text{where} \\
 N_t^{ic}|n_0 &\sim \text{Bin}(n_0, e^{-\lambda t}), \\
 N_t^s &\sim \text{Poi}\left(\frac{\mu}{\lambda} (1 - e^{-\lambda t})\right).
 \end{aligned} \tag{38}$$

Hence as  $t \rightarrow \infty$ , the distribution will tend towards  $\text{Poi}(\mu/\lambda)$ , the stationary distribution of the population. This is a well-known result in the literature [16, 6].

##### Starting at stationarity: the time-dependent $N_t^{ic}$ and $N_t^s$ balance each other at all times

It is illustrative to consider the dynamics of this system when the initial condition is chosen to be the stationary distribution. In this case, the breakdown of  $N_t$  into the time-dependent components  $N_t^{ic}$  and

$N_t^s$  will need to reproduce the stationary distribution at all times  $t > 0$ , with no ‘burn-in’ period.

To see this, let the initial distribution start at stationarity, i.e.,  $N_0 \sim \text{Poi}(\mu/\lambda)$  and

$$\Pr(N_0 = n_0) = \left(\frac{\mu}{\lambda}\right)^{n_0} \frac{e^{-\mu/\lambda}}{n_0!}.$$

The distribution of  $N_t^s$  is still given by (38) and the contribution of  $N_t^{ic}$  is given by

$$\begin{aligned} \Pr(N_t^{ic} = k) &= \sum_{n_0=k}^{\infty} \Pr(N_t^{ic} = k | N_0 = n_0) \Pr(N_0 = n_0) \\ &= \sum_{n_0=k}^{\infty} \binom{n_0}{k} (e^{-\lambda t})^k (1 - e^{-\lambda t})^{n_0-k} \left(\frac{\mu}{\lambda}\right)^{n_0} \frac{e^{-\mu/\lambda}}{n_0!} = (e^{-\lambda t})^k e^{-\mu/\lambda} \sum_{r=0}^{\infty} \left(\frac{\mu}{\lambda}\right)^{r+k} \frac{(1 - e^{-\lambda t})^r}{k! r!} \\ &= \left(\frac{\mu}{\lambda}\right)^k \frac{(e^{-\lambda t})^k e^{-\mu/\lambda}}{k!} \sum_{r=0}^{\infty} \left(\frac{\mu}{\lambda}\right)^r \frac{(1 - e^{-\lambda t})^r}{r!} = \left(\frac{\mu}{\lambda}\right)^k \frac{(e^{-\lambda t})^k e^{-\mu/\lambda}}{k!} e^{\frac{\mu}{\lambda}(1 - e^{-\lambda t})} = \left(\frac{\mu}{\lambda} e^{-\lambda t}\right)^k \frac{e^{-\frac{\mu}{\lambda} e^{-\lambda t}}}{k!}. \end{aligned}$$

In other words,  $N_t^{ic} \sim \text{Poi}\left(\frac{\mu}{\lambda} e^{-\lambda t}\right)$ , which cancels the contribution from  $N_t^s \sim \text{Poi}\left(\frac{\mu}{\lambda} [1 - e^{-\lambda t}]\right)$ . Therefore

$$N_t \sim \text{Poi}\left(\frac{\mu}{\lambda}\right), \quad \forall t.$$

This example shows that  $N_t^{ic}$  and  $N_t^s$  will combine to reproduce a stationary distribution at all times  $t > 0$ , when the system starts at stationarity so that there is no ‘burn-in’ transient.

### Starting the system at $t = -\infty$

The same is true if the system is not stationary but we start the system at  $t = -\infty$  with any initial condition. Then, for  $t > 0$ , the system will be independent of the initial condition and will be described by  $N_t^s$ .

Let us denote the state of the system for  $t > 0$  by the *attracting* distribution  $P_*$ . Although  $\Pr(N_t^s = n) = P_*(n, t), \forall n \in \mathbb{N}, \forall t > 0$ , we wish to distinguish  $P_*$  from  $P_s$  because we only have equality of the two distributions when the system starts at  $t = -\infty$ .  $P_*$  can be thought of as an inherent property of the system, analogous to the stable point of a dynamical system that moves in time (sometimes called a *chronotaxic system* [61]).

If  $\Pr(N_0 = n_0) = P_*(n_0, 0)$  for all  $n_0$  in Eq. (9), the contributions from  $N_t^{ic}$  and  $N_t^s$  balance each other as they did in the case of stationarity with  $N_0 \sim \text{Poi}(\mu/\lambda)$ , and we would have  $P(n, t) = P_*(n, t), \forall n \in \mathbb{N}, \forall t > 0$  (recall that the breakdown  $N_t = N_t^{ic} + N_t^s$  simply resolves the existing mRNA molecules into those that were present at  $t = 0$ , and those that were transcribed since  $t = 0$ ). Thus we only observe an initial transient period if the initial distribution starts away from its attracting distribution at  $t = 0$ . In all other cases, the following mathematical formulations are equivalent: *i*) assume that the system was initialised at  $t = -\infty$  and consider only  $N_t^s$ , or *ii*) use the initial distribution  $P_*(n, 0)$  for all  $n$  at  $t = 0$ , and consider  $N_t^{ic} + N_t^s$ .

In this work, we focus on the time dependence of  $P(n, t)$  induced through non-stationarity of the parameters, and/or synchronous behaviour of the cells within the population. Hence, unless otherwise stated, in this work we assume that the system was initialised at  $t = -\infty$  and that the distribution of  $N_t^s$  is the attracting distribution  $P_*(n, t)$  for all  $t > 0$ , i.e., we neglect the contribution from  $N_t^{ic}$ .

## A.2 ‘Burn-in’ transience in the random telegraph model

A time-dependent solution of the probability generating function for the random telegraph model appeared in Ref. [21], although the explicit expression for  $P(n, t)$  was omitted. As discussed above, the RT model represents asynchronous and stationary behaviour, hence the time-dependence appears only through convergence to the stationary distribution from the initial condition. We include the derivation here for completeness and to complement Fig. 7.

Consider the RT model depicted in Fig. 3a. Assuming that every cell is initialised in the inactive state with  $n_0 = 0$  mRNA molecules, the probability generating function for the cell population is [21]:

$$G(z, t) = F_s(z, t)\Phi_s(z, t) - \frac{\mu k_{\text{on}} e^{-(k_{\text{on}} + k_{\text{off}})t}}{(k_{\text{on}} + k_{\text{off}})(1 - k_{\text{on}} - k_{\text{off}})} (1 - z)F_{ns}(z, t)\Phi_{ns}(z, t)$$

where  $F_s(z, t) := {}_1F_1[-k_{\text{on}}, 1 - k_{\text{on}} - k_{\text{off}}; \mu e^{-t}(1 - z)]$ ,  $\Phi_s(z, t) := {}_1F_1[k_{\text{on}}, k_{\text{on}} + k_{\text{off}}; -\mu(1 - z)]$ ,  $F_{ns}(z, t) := {}_1F_1[k_{\text{off}}, 1 + k_{\text{on}} + k_{\text{off}}; \mu e^{-t}(1 - z)]$ , and  $\Phi_{ns}(z, t) := {}_1F_1[1 - k_{\text{off}}, 2 - k_{\text{on}} - k_{\text{off}}; -\mu(1 - z)]$ . Here  ${}_1F_1(a, b; z)$  is the confluent hypergeometric function [1].

Using the general Leibniz rule for differentiation, and omitting other details of the differentiation, we obtain

$$\begin{aligned} P(n, t) &= \frac{1}{n!} \frac{\partial^n G}{\partial z^n} \Big|_{z=0} \\ &= \frac{\mu^n}{n!} \sum_{r=0}^n \binom{n}{r} \frac{(-1)^r (-k_{\text{on}})_r (k_{\text{on}})_{n-r} e^{-rt}}{(1 - k_{\text{on}} - k_{\text{off}})_r (k_{\text{on}} + k_{\text{off}})_{n-r}} {}_1F_1[-k_{\text{on}} + r, 1 - k_{\text{on}} - k_{\text{off}} + r; \mu e^{-t}] \\ &\quad \times {}_1F_1[k_{\text{on}} + n - r, k_{\text{on}} + k_{\text{off}} + n - r; -\mu] \\ &+ \frac{k_{\text{on}} \mu^{n+1} e^{-(k_{\text{on}} + k_{\text{off}})t}}{(k_{\text{on}} + k_{\text{off}})(1 - k_{\text{on}} - k_{\text{off}})n!} \sum_{r=0}^n \binom{n}{r} \frac{(-1)^r (-k_{\text{off}})_r (1 - k_{\text{off}})_{n-r} e^{-rt}}{(1 + k_{\text{on}} + k_{\text{off}})_r (2 - k_{\text{on}} - k_{\text{off}})_{n-r}} \\ &\quad \times {}_1F_1[k_{\text{off}} + r, 1 + k_{\text{on}} + k_{\text{off}} + r; \mu e^{-t}] {}_1F_1[1 - k_{\text{off}} + n - r, 2 - k_{\text{on}} - k_{\text{off}} + n - r; -\mu] \\ &- \frac{k_{\text{on}} \mu^n e^{-(k_{\text{on}} + k_{\text{off}})t}}{(k_{\text{on}} + k_{\text{off}})(1 - k_{\text{on}} - k_{\text{off}})n!} \sum_{r=0}^{n-1} \binom{n-1}{r} \frac{(-1)^r (-k_{\text{off}})_r (1 - k_{\text{off}})_{n-1-r} e^{-rt}}{(1 + k_{\text{on}} + k_{\text{off}})_r (2 - k_{\text{on}} - k_{\text{off}})_{n-1-r}} \\ &\quad \times {}_1F_1[k_{\text{off}} + r, 1 + k_{\text{on}} + k_{\text{off}} + r; \mu e^{-t}] {}_1F_1[-k_{\text{off}} + n - r, 1 - k_{\text{on}} - k_{\text{off}} + n - r; -\mu], \end{aligned}$$

where  $(a)_m := a(a+1)\dots(a+m-1)$  is Pochhammer’s function [1].

As  $\zeta \rightarrow 0$ ,  ${}_1F_1[a, b; \zeta] \rightarrow 1$ . Hence as  $t \rightarrow \infty$ ,  $P(n, t) \rightarrow P(n)$ , and we recover the known stationary solution:

$$P(n) = \frac{\mu^n}{n!} \frac{(k_{\text{on}})_n}{(k_{\text{on}} + k_{\text{off}})_n} {}_1F_1[k_{\text{on}} + n, k_{\text{on}} + k_{\text{off}} + n; -\mu].$$

## B The stationary solution for the refractory promoter model (3 cyclic promoter states)

As explained in Section 3.2.2, the stationary solution of the 3-state cyclic model describing a refractory promoter is obtained by solving the set of equations:

$$\frac{d}{dz} [(1-z)f_*(z)] = -k_*f_*(z) + k_2f_2(z) \quad (39)$$

$$\frac{d}{dz} [-zf_1(z)] = -k_1f_1(z) + k_*f_*(z) \quad (40)$$

$$\frac{d}{dz} [-zf_2(z)] = -k_2f_2(z) + k_1f_1(z) \quad (41)$$

to obtain an expression for  $f_Z = f_* + f_1 + f_2$ .

Note that the transition matrix  $[k_{sr}]$  containing the kinetic constants on the right-hand side of Eqs (39)-(41) is singular and hence  $\lambda = 0$  is an eigenvalue. Furthermore, by Gershgorin's circle theorem the non-zero eigenvalues of  $[k_{sr}]$  have negative real parts, so a stationary solution always exists, i.e., the probabilities  $\pi_i = \int_x f_i(x) dx$  of being in state  $S_i$  evolve to an equilibrium state given by the eigenvector  $\hat{\pi}$  associated with the eigenvalue  $\lambda = 0$ . Note that  $\hat{\pi}$  must be normalised so that the elements sum to 1. It can easily be shown that

$$\pi_i = \int_0^1 f_i(z) dz = \frac{k_1k_2k_*}{k_i(k_2k_* + k_1k_* + k_1k_2)}. \quad (42)$$

Now, integrating Eqs (39)-(41) and using Eq. (42) we obtain the boundary values  $f_1(1) = f_2(1) = 0$  and  $f_*(0) = 0$ . Also, summing Eqs (39)-(41) and integrating gives

$$-zf_1(z) - zf_2(z) + (1-z)f_*(z) = C, \quad (43)$$

where  $C$  is a constant. Eq. (43) is true for all  $z \in [0, 1]$ , so we can substitute in  $z = 0$  or  $z = 1$  and use the fact that  $f_1(1) = 0$  and  $f_1(1) = 0$ , or  $f_*(0) = 0$ , to show that  $C = 0$ . Hence

$$f_Z(z) = f_1(z) + f_2(z) + f_*(z) = \frac{1}{z}f_*(z), \quad (44)$$

so we need only solve Eqs (39)-(41) for  $f_*(z)$ , the marginal probability density corresponding to the active state. Using (44) and substituting into (39)-(41), we then obtain the following equation for  $f_*(z)$ :

$$\begin{aligned} 0 = & z^2(1-z)f_*''(z) + z[(-3 + k_1 + k_2 + k_*)z + 1 - k_1 - k_2]f_*'(z) \\ & + [(-1 + k_1 + k_2 - k_1k_2 - k_1k_*)z + k_1k_2]f_*(z). \end{aligned} \quad (45)$$

Set  $f(z) = z^cu(z)$ , where  $c$  is a constant that we can choose, to transform (45) into

$$\begin{aligned} 0 = & z^{c+2}(1-z)u''(z) + z^{c+1}[(-3 + \mathcal{K} - 2c)z + 1 - k_1 - k_2 + 2c]u'(z) \\ & + z^c[(-1 + \mathcal{K} - \tilde{\mathcal{K}} + (-2 + \mathcal{K} - c)c)z + k_1k_2 - (k_1 + k_2)c + c^2]u(z) \end{aligned}$$

where  $\mathcal{K} := k_1 + k_2 + k_*$  and  $\tilde{\mathcal{K}} := k_1 k_2 + k_1 k_* + k_2 k_*$ . From here, we set the last term on the right hand side to zero by choosing  $c = k_1$  or  $c = k_2$ . We can then divide through by  $z^{c+1}$  to obtain an equation in the form of the hypergeometric equation [1]. For example, for  $c = k_1$  we obtain

$$0 = z(1-z)u''(z) + [(-3 - k_1 + k_2 + k_*)z + 1 + k_1 - k_2]u'(z) + [-1 - k_1 + k_2 + k_* - k_2 k_*]u(z).$$

When none of  $\sqrt{(k_1 - k_2 - k_*)^2 - 4k_2 k_*}$ ,  $k_1 - k_2$ , or  $k_*$  are integers, we can write down the solution [1]:

$$u(z) = C_1 {}_2F_1 \left[ a_+^{(1)}, a_-^{(1)}; 1 + k_1 - k_2; z \right] + C_2 z^{-k_1+k_2} {}_2F_1 \left[ a_+^{(2)}, a_-^{(2)}; 1 - k_1 + k_2; z \right]$$

where  $C_1$  and  $C_2$  are constants of integration,  ${}_2F_1[a, b; c; z]$  is the Gauss hypergeometric function [1], and

$$a_{\pm}^{(1)} = \frac{1}{2} \left( 2 + k_1 - k_2 - k_* \pm \sqrt{(k_* - k_1 - k_2)^2 - 4k_1 k_2} \right) \\ a_{\pm}^{(2)} = \frac{1}{2} \left( 2 - k_1 + k_2 - k_* \pm \sqrt{(k_* - k_1 - k_2)^2 - 4k_1 k_2} \right).$$

The solutions for the other cases are similar and are also given in [1]. Hence  $f_*(z) = z^{k_1}u(z)$  is given by

$$f_*(z) = C_1 z^{k_1} {}_2F_1 \left[ a_+^{(1)}, a_-^{(1)}; 1 + k_1 - k_2; z \right] + C_2 z^{k_2} {}_2F_1 \left[ a_+^{(2)}, a_-^{(2)}; 1 - k_1 + k_2; z \right].$$

The same expression for  $f_*(z)$  is obtained if we choose  $c = k_2$  instead, so finally we can write down the general solution for  $f_Z(z) = f_*(z)/z$ :

$$f_Z(z) = C_1 z^{k_1-1} {}_2F_1 \left[ a_+^{(1)}, a_-^{(1)}; 1 + k_1 - k_2; z \right] + C_2 z^{k_2-1} {}_2F_1 \left[ a_+^{(2)}, a_-^{(2)}; 1 - k_1 + k_2; z \right] \\ = C_1 z^{k_1-1} (1-z)^{k_*-1} {}_2F_1 \left[ a_+^{(1)} + k_* - 1, a_-^{(1)} + k_* - 1; 1 + k_1 - k_2; z \right] \\ + C_2 z^{k_2-1} (1-z)^{k_*-1} {}_2F_1 \left[ a_+^{(2)} + k_* - 1, a_-^{(2)} + k_* - 1; 1 - k_1 + k_2; z \right]. \quad (46)$$

Here,  $C_1$  and  $C_2$  are normalising constants that ensure the integral constraints

$$\int_0^1 f_*(z) dz = \pi_* \\ \int_0^1 f_Z(z) dz = \int_0^1 \frac{1}{z} f_*(z) dz = 1$$

are satisfied. These constants are conveniently obtained from a Mellin transform identity (see Ref. [56], p. 152):

$$C_1 = \frac{\Gamma(k_2 - k_1)}{\Gamma(k_1)\Gamma(k_2)} \frac{\Gamma(1 + k_1 - a_+^{(1)})}{\Gamma(1 - a_+^{(1)})} \frac{\Gamma(1 + k_1 - a_-^{(1)})}{\Gamma(1 - a_-^{(1)})}; \\ C_2 = \frac{\Gamma(k_1 - k_2)}{\Gamma(k_1)\Gamma(k_2)} \frac{\Gamma(1 + k_2 - a_+^{(2)})}{\Gamma(1 - a_+^{(2)})} \frac{\Gamma(1 + k_2 - a_-^{(2)})}{\Gamma(1 - a_-^{(2)})},$$

where  $\Gamma(\cdot)$  is the Gamma function [1]. Eq. (46) is useful for comparisons with the 2-state random telegraph model.